TDDFT and Quantum-Classical Dynamics: a Universal Tool Describing the Dynamics of Matter

Federica Agostini[1], Basile F. E. Curchod[2], Rodolphe Vuilleumier[3a,3b], Ivano Tavernelli[4], E. K. U. Gross[5]

Abstract Time-dependent density functional theory (TDDFT) is currently the most efficient approach allowing to describe electronic dynamics in complex systems, from isolated molecules to the condensed-phase. TDDFT has been employed to investigate an extremely wide range of time-dependent phenomena, as spin dynamics in solids, charge and energy transport in nanoscale devices, and photoinduced exciton transfer in molecular aggregates. It is therefore nearly impossible to give a general account of all developments and applications of TDDFT in material science, as well as in physics and chemistry. A large variety of aspects are covered throughout these volumes, see e.g. Chapters X, Y (to be indicated). In the present chapter, we will limit our presentation to the description of TDDFT developments and applications in the field of quantum molecular dynamics simulations in combination with trajectory-based approaches for the study of nonadiabatic excited-state phenomena. We will present different quantum-classical strategies used to describe the coupled dynamics of electrons and nuclei underlying nonadiabatic processes. In addition, we will give an account of the most recent applications with the aim of illustrating the nature of the problems that can be addressed with the help of these approaches. The potential, as well as the limitations, of the presented methods are discussed,

[1]Laboratoire de Chimie Physique, UMR 8000 CNRS/University Paris-Sud, University Paris-Saclay, 91405 Orsay, France, e-mail: federica.agostini@u-psud.fr
[2]Department of Chemistry, Durham University, South Road, Durham DH1 3LE, United Kingdom, e-mail: basile.f.curchod@durham.ac.uk
[3a]PASTEUR, Département de chimie, École normale supérieure, UPMC Univ. Paris 06, CNRS, PSL Research University, 75005 Paris, France.
[3b]Sorbonne Universités, UPMC Univ. Paris 06, École normale suprieure, CNRS, Processus d'activation sélective par transfert d'énergie uni-électronique ou radiatif (PASTEUR), 75005 Paris, France, e-mail: rodolphe.vuilleumier@ens.fr
[4]Zurich Research Laboratory, IBM Research GmbH, 8803 Rüschlikon, Switzerland, e-mail: ita@zurich.ibm.com
[5]Max-Planck-Institut für Mikrostrukturphysik, Weinberg 2, Halle 06120, Germany, e-mail: hardy@mpi-halle.mpg.de

along with possible avenues for future developments in TDDFT and nonadiabatic dynamics.

1 Introduction

Photoinduced isomerization processes, photosynthetic and photovoltaic energy conversion phenomena, charge and energy transport through molecular junctions, are all typical examples of, so-called, nonadiabatic processes. Nonadiabatic processes are characterized by a strong coupling between electronic and nuclear motion; in fact, nuclear motion is responsible for inducing electronic (nonadiabatic) transitions, and in turn, the time evolution of the electronic states also affects the nuclear dynamics at very short timescales (down to a few tens of fs). In this nonadiabatic regime, thus when the Born-Oppenheimer approximation breaks down, performing (quantum) molecular dynamics simulations is tremendously challenging. Accurate electronic structure properties are required to describe electronic dynamics, and to correctly *drive* the nuclear evolution. Identifying regions of nuclear configuration space where the electronic states are coupled, as avoided crossings and conical intersections, is essential to predict quantum yields. Efficient evolution techniques have to be employed to describe nuclear motion in order, for instance, to determine final molecular structures, or to account for possible quantum effects. Therefore, theoretical and numerical developments need to address the problem from the perspective of both electronic structure theory and nuclear quantum dynamics.

Perhaps the most celebrated method to investigate excited electronic states is time-dependent density functional theory (TDDFT). TDDFT offers an in principle exact formalism for propagating the time-dependent electronic density and, within linear response theory, for calculating excitation energies as well as critical excited-state properties. It is therefore without any surprise that TDDFT became the electronic-structure method of choice to be coupled with nonadiabatic dynamics. Particularly successful has been the combination of TDDFT, employed to solve the electronic problem, with the description of nuclear motion in terms of trajectories that evolve or hop between coupled (electronic) potential energy surfaces. The most well-known method is Tully's "fewest switches" trajectory surface hopping (Tully (1990)), which has evolved into a widely used and successful technique. The mean-field Ehrenfest dynamics is often employed to investigate explicitly the electronic dynamics, combined for example with real-time TDDFT Tavernelli et al (2005); Tavernelli (2006). Full multiple spawning (Martínez et al (1996); Martínez and Levine (1997); Ben-Nun and Martínez (1998); Ben-Nun et al (2000); Hack et al (2001); Ben-Nun and Martínez (2002); Virshup et al (2008)) propagates coupled Gaussian functions along classical trajectories, whereas the coupled-trajectory mixed quantum-classical (CT-MQC) scheme (Min et al (2015)) derived from the Exact Factorization (Abedi et al (2010)) is based on the propagation of trajectories along a time-dependent potential energy surface (Abedi et al (2013a)). Other techniques like the quantum-classical Liouville equation (Kapral and Ciccotti (1999);

Nielsen et al (2000); Kapral (2006)), Bohmian dynamics (Wyatt et al (2001); Lopreore and Wyatt (2002); Rassolov and Garashchuk (2005); Curchod and Tavernelli (2013a)), variational multiconfiguration Gaussians (Worth et al (2004); Lasorne et al (2006, 2007); Worth et al (2008); Mendive-Tapia et al (2012); Richings et al (2015)), multiconfigurational Ehrenfest (Shalashilin (2010); Saita and Shalashilin (2012); Makhov et al (2017)) or linearization approaches to compute time-correlations functions (Bonella and Coker (2005); Huo and Coker (2012); Dunkel et al (2008)) have been also proposed for nonadiabatic dynamics. Despite their differences, all the methods mentioned above are rooted in the Born-Huang representation of the total molecular wavefunction, i.e., an expansion in an infinite sum over the correlated Born-Oppenheimer electronic states. In contrast, the recently introduced Exact Factorization of the time-dependent molecular wavefunction offers a paradigm shift in our perception of nonadiabatic dynamics, away from the Born-Huang picture, and blaze a trail for the development of nonadiabatic techniques away from Born-Oppenheimer concepts. It is important to mention here that ensembles of trajectories, when properly constructed via the method of characteristics (Agostini et al (2018)), can represent, in principle arbitrarily closely, the solution of the underlying partial differential equation. Practical implementations, however, involve further-going approximations where, for instance, interference and tunnelling effects are neglected or only approximately taken into account. The advantage of trajectory-based method is that they circumvent the enormous numerical effort associated with quantum wavepackets propagation techniques, such as Multi Configuration Time Dependent Hartree approach (MCTDH) (Meyer et al (1990); Burghardt et al (1999); Wang and Thoss (2003); Meyer and Worth (2003)). By its very nature, this approach requires the computation of the relevant potential energy surfaces (PESs) and corresponding couplings before the actual propagation of nuclear wavepackets. This clearly implies an important computational effort that limits the applicability of this method to a small number of degrees of freedom (up to ~ 10). In addition, the determination of the relevant degrees of freedom to include in the dynamics can also become a challenging problem, which requires some *a priori* knowledge of the "active" vibrational modes involved in the dynamics. Such wavefucntion-based nonadiabatic approaches are beyond the scope of this chapter and will not be discussed further.

The goal of this chapter is to present in a self-contained manner the key theoretical concepts and equations of the most important methods cited above, starting from the electronic structure problem and (LR-)TDDFT, up to nuclear dynamics methods like Surface Hopping, Ehrenfest dynamics, and Ab Initio Multiple Spawning. To contrast with these Born-Huang-based methods, we also present the formalism of the Exact Factorization and introduce the reader to the first mixed-quantum classical algorithm derived from this formalism, coined coupled-trajectory mixed quantum classical (CT-MQC) dynamics.

2 Coupled electron-nuclear dynamics in molecules

In molecules and condensed phase systems, the time evolution of interacting electrons and nuclei is described by the time-dependent Schrödinger equation

$$\hat{H}\Psi(\mathbf{r},\mathbf{R},t) = i\hbar\partial_t\Psi(\mathbf{r},\mathbf{R},t)\,, \tag{1}$$

where the electron-nuclear wavefunction $\Psi(\mathbf{r},\mathbf{R},t)$ describes the state of the system over time, and $\hat{H}$ is the molecular Hamiltonian, i.e.,

$$\begin{aligned}\hat{H}(\mathbf{r},\mathbf{R}) &= \sum_{\nu=1}^{N_n}\frac{-\hbar^2}{2M_\nu}\nabla_\nu^2 + \hat{T}_e(\mathbf{r}) + V_{ee}(\mathbf{r}) + V_{nn}(\mathbf{R}) + V_{en}(\mathbf{r},\mathbf{R}) \\ &= \sum_{\nu=1}^{N_n}\frac{-\hbar^2}{2M_\nu}\nabla_\nu^2 + \hat{H}_{BO}(\mathbf{r},\mathbf{R})\,. \end{aligned} \tag{2}$$

Here, $\mathbf{r} = (\mathbf{r}_1,\ldots,\mathbf{r}_{N_{el}})$, $\mathbf{R} = (\mathbf{R}_1,\ldots,\mathbf{R}_{N_n})$, N_{el} is the number of electrons and N_n the number of nuclei. The first term on the right-hand side of Eq. (2) is the nuclear kinetic energy, with ∇_ν indicating the spatial derivative with respect to the position of the nucleus ν, and M_ν its mass, whereas $\hat{H}_{BO}$ is the so-called Born-Oppenheimer (BO), or electronic, Hamiltonian. $\hat{H}_{BO}$ is defined as the sum of the electronic kinetic energy, $\hat{T}_e$, the electron-electron, $\hat{V}_{ee}$, the nucleus-nucleus V_{nn}, and the electron-nucleus, V_{en}, interactions.

Usually, the problem is reformulated adopting the Born-Huang expansion of the molecular wavefunction in the adiabatic basis. The adiabatic, or BO, states, $\varphi_{\mathbf{R}}^{(k)}(\mathbf{r})$, are defined as the eigenfunctions of the BO Hamiltonian,

$$\hat{H}_{BO}(\mathbf{r},\mathbf{R})\varphi_{\mathbf{R}}^{(k)}(\mathbf{r}) = \varepsilon_{BO}^{(k)}(\mathbf{R})\varphi_{\mathbf{R}}^{(k)}(\mathbf{r})\,, \tag{3}$$

with eigenvalues $\varepsilon_{BO}^{(k)}(\mathbf{R})$. The electronic time-independent problem is diagonalized at each nuclear position $\mathbf{R}$, thus the eigenfunctions and eigenvalues depend on $\mathbf{R}$. Nuclear positions are interpreted here as parameters, that label both the electronic states and the electronic energies. If Eq. (3) is solved for all nuclear configurations, $\varepsilon_{BO}^{(k)}(\mathbf{R})$ identify the so-called BO potential energy surfaces (PESs). In the Born-Huang expansion of the electron-nuclear wavefunction,

$$\Psi(\mathbf{r},\mathbf{R},t) = \sum_k \chi_k(\mathbf{R},t)\varphi_{\mathbf{R}}^{(k)}(\mathbf{r})\,, \tag{4}$$

the coefficients $\chi_k(\mathbf{R},t)$ clearly depend on nuclear positions and on time. These coefficients can be interpreted as the nuclear contributions corresponding to the electronic states included in the sum, and can be also referred to as nuclear wavepackets. In fact, it can be easily proven that the nuclear density, defined as the integral of $|\Psi(\mathbf{r},\mathbf{R},t)|^2$ over electronic coordinates,

$$\int d\mathbf{r}\,|\Psi(\mathbf{r},\mathbf{R},t)|^2 = \sum_k |\chi_k(\mathbf{R},t)|^2\,, \tag{5}$$

can be written as the sum of adiabatic contributions, $|\chi_k(\mathbf{R},t)|^2$. Here, the orthogonality of the BO states

$$\int d\mathbf{r}\varphi_{\mathbf{R}}^{(l)^*}(\mathbf{r})\varphi_{\mathbf{R}}^{(k)}(\mathbf{r}) = \left\langle \varphi_{\mathbf{R}}^{(l)} \middle| \varphi_{\mathbf{R}}^{(k)} \right\rangle_{\mathbf{r}} = \delta_{lk} \tag{6}$$

has been used.

The Born-Huang expansion (4) is inserted in Eq. (1), that is then projected on $\varphi_{\mathbf{R}}^{(k)^*}(\mathbf{r})$ and integrated over $\mathbf{r}$. A set of partial differential equations are derived for the expansion coefficients

$$\left[\sum_{\nu}^{N_n} \frac{-\hbar^2}{2M_\nu}\nabla_\nu^2 + \varepsilon_{BO}^{(k)}(\mathbf{R})\right]\chi_k(\mathbf{R},t) + \sum_l \mathscr{F}_{kl}(\mathbf{R})\chi_l(\mathbf{R},t) = i\hbar\partial_t\chi_k(\mathbf{R},t)\,. \tag{7}$$

The last term on the right-hand side is responsible for coupling the evolution of the k-th coefficient to all other coefficients, via the nonadiabatic couplings

$$\begin{aligned}\mathscr{F}_{kl}(\mathbf{R}) = &\int d\mathbf{r}\;\varphi_{\mathbf{R}}^{(k)^*}(\mathbf{r})\left[\sum_{\nu}^{N_n}\frac{-\hbar^2}{2M_\nu}\nabla_\nu^2\right]\varphi_{\mathbf{R}}^{(l)}(\mathbf{r}) \\ &+\sum_{\nu}^{N_n}\frac{1}{M_\nu}\left\{\int d\mathbf{r}\;\varphi_{\mathbf{R}}^{(k)^*}(\mathbf{r})\left[-i\hbar\nabla_\nu\varphi_{\mathbf{R}}^{(l)}(\mathbf{r})\right]\right\}\cdot\left[-i\hbar\nabla_\nu\right]\,,\end{aligned} \tag{8}$$

arising from the effect of the nuclear kinetic energy operator on the parametric dependence of the BO states on $\mathbf{R}$. In the most general case, the non-diagonal elements of $\mathscr{F}_{kl}(\mathbf{R})$ are non-zero and induce a coupling between different electronic states due to the motion of the nuclei. The nonadiabatic coupling term is responsible for exchanging "nuclear contributions" between the electronic adiabatic states k and l. The BO framework presented so far is widely adopted by a large community of physicists and chemists to interpret the coupled electron-nuclear problem under nonadiabatic conditions. However, such framework is not the only one, as we will discuss below.

An alternative perspective on the coupled electron-nuclear problem has been recently proposed, the Exact Factorization of the electron-nuclear wavefunction (Abedi et al (2010, 2012)). In this framework, we make an Ansatz different from the Born-Huang representation of the molecular wavefunction, namely

$$\Psi(\mathbf{r},\mathbf{R},t) = \Phi_{\mathbf{R}}(\mathbf{r},t)\chi(\mathbf{R},t)\,. \tag{9}$$

Here $\chi(\mathbf{R},t)$ is the nuclear wavefunction and $\Phi_{\mathbf{R}}(\mathbf{r},t)$ is the electronic wavefunction which parametrically depends on the nuclear positions and satisfies the partial normalization condition (PNC)

$$\int d\mathbf{r}\,|\Phi_{\mathbf{R}}(\mathbf{r},t)|^2 = 1 \quad \forall\,\mathbf{R},t\,. \tag{10}$$

The theorems introduced in (Abedi et al (2010, 2012)) prove the existence and uniqueness of Eq. (9), up to within a $(\mathbf{R},t)$-dependent gauge transformation. The PNC guarantees the interpretation of $|\chi(\mathbf{R},t)|^2$ as the probability of finding the nuclear configuration $\mathbf{R}$ at time t, and of $|\Phi_{\mathbf{R}}(\mathbf{r},t)|^2$ itself as the conditional probability of finding the electronic configuration $\mathbf{r}$ at time t given the nuclear configuration $\mathbf{R}$.

The stationary variations (Frenkel (1934)) of the quantum mechanical action with respect to $\Phi_{\mathbf{R}}(\mathbf{r},t)$ and $\chi(\mathbf{R},t)$ lead to the derivation of the following equations of motion

$$\left(\hat{H}_{BO}(\mathbf{r},\mathbf{R}) + \hat{U}_{en}^{coup}[\Phi_{\mathbf{R}},\chi] - \varepsilon(\mathbf{R},t)\right)\Phi_{\mathbf{R}}(\mathbf{r},t) = i\hbar\partial_t\Phi_{\mathbf{R}}(\mathbf{r},t) \tag{11}$$

$$\left[\sum_{\nu=1}^{N_n}\frac{\left[-i\hbar\nabla_\nu + \mathbf{A}_\nu(\mathbf{R},t)\right]^2}{2M_\nu} + \varepsilon(\mathbf{R},t)\right]\chi(\mathbf{R},t) = i\hbar\partial_t\chi(\mathbf{R},t), \tag{12}$$

where the PNC is enforced by means of Lagrange multipliers (Alonso et al (2013); Abedi et al (2013b)). The electron-nuclear coupling operator (Agostini et al (2015b)),

$$\hat{U}_{en}^{coup}[\Phi_{\mathbf{R}},\chi] = \sum_{\nu=1}^{N_n}\frac{1}{M_\nu}\left[\frac{\left[-i\hbar\nabla_\nu - \mathbf{A}_\nu(\mathbf{R},t)\right]^2}{2}\right.$$
$$\left. + \left(\frac{-i\hbar\nabla_\nu\chi}{\chi} + \mathbf{A}_\nu(\mathbf{R},t)\right)\left(-i\hbar\nabla_\nu - \mathbf{A}_\nu(\mathbf{R},t)\right)\right], \tag{13}$$

the time-dependent potential energy surface (TDPES) (Abedi et al (2013a); Agostini et al (2013); Suzuki et al (2015); Agostini et al (2015a); Curchod et al (2016a); Suzuki and Watanabe (2016)),

$$\varepsilon(\mathbf{R},t) = \langle\Phi_{\mathbf{R}}(t)|\,\hat{H}_{BO} + \hat{U}_{en}^{coup} - i\hbar\partial_t\,|\Phi_{\mathbf{R}}(t)\rangle_{\mathbf{r}}\,, \tag{14}$$

and the time-dependent vector potential (Curchod and Agostini (2017)),

$$\mathbf{A}_\nu(\mathbf{R},t) = \langle\Phi_{\mathbf{R}}(t)|-i\hbar\nabla_\nu\,\Phi_{\mathbf{R}}(t)\rangle_{\mathbf{r}} \tag{15}$$

are responsible for the coupling between electrons and nuclei in a formally exact way. It is worth noting that the electron-nuclear coupling operator, $\hat{U}_{en}^{coup}[\Phi_{\mathbf{R}},\chi]$, in the electronic equation (11), depends on the nuclear wavefunction and acts on the parametric dependence of $\Phi_{\mathbf{R}}(\mathbf{r},t)$ as a differential operator. This "pseudo-operator" includes the coupling to the nuclear subsystem beyond the parametric dependence in the BO Hamiltonian $\hat{H}_{BO}(\mathbf{r},\mathbf{R})$. The symbol $\langle\,\cdot\,\rangle_{\mathbf{r}}$ indicates an integration over electronic coordinates only. The nuclear equation (12) has the particularly appealing form of a Schrödinger equation that contains a time-dependent vector potential (15) and a time-dependent scalar potential (14) that govern the nuclear dynamics and yield the nuclear wavefunction. $\chi(\mathbf{R},t)$ is interpreted as the nuclear wavefunction since it leads to an N-body nuclear density, and an N-body current-density, which

reproduce the true nuclear N-body density and current-density (Abedi et al (2012)) obtained from the full wavefunction $\Psi(\mathbf{r},\mathbf{R},t)$.

In order to connect the Born-Huang representation to the Exact Factorization, the electronic wavefunction $\Phi_{\mathbf{R}}(\mathbf{R},t)$ is expanded in terms of the BO states, similarly to what is done for the molecular wavefunction of Eq. (4), namely

$$\Phi_{\mathbf{R}}(\mathbf{r},t) = \sum_k C_k(\mathbf{R},t)\varphi_{\mathbf{R}}^{(k)}(\mathbf{r}). \tag{16}$$

The expansion coefficients in Eqs. (4) and (16) are related,

$$\chi_k(\mathbf{R},t) = C_k(\mathbf{R},t)\chi(\mathbf{R},t), \tag{17}$$

by virtue of the factorization (9). Additionally, the PNC can be rewritten as

$$\sum_k |C_k(\mathbf{R},t)|^2 = 1 \quad \forall\, \mathbf{R},t. \tag{18}$$

We point out that even in the case where the nuclear wavepacket splits into more than one BO PESs the full wavefunction is still a single product: the nuclear wavefunction has contributions (projections) on different BO PESs while the electronic wavefunction is a linear combination of the adiabatic states, but still we may write

$$\Psi(\mathbf{r},\mathbf{R},t) = \left(e^{\frac{i}{\hbar}S(\mathbf{R},t)}\sqrt{\sum_l |\chi_l(\mathbf{R},t)|^2}\right)\left(\sum_k C_k(\mathbf{R},t)\varphi_{\mathbf{R}}^{(k)}(\mathbf{r})\right) \tag{19}$$

where the first term in parenthesis is $\chi(\mathbf{R},t)$, with a phase $S(\mathbf{R},t)$ determined by fixing the gauge freedom, and the second term in parenthesis is $\Phi_{\mathbf{R}}(\mathbf{r},t)$, using Eq. (16).

In the absence of nonadiabatic couplings in Eq. (7), the evolution equations for the coefficients $\chi_k(\mathbf{R},t)$ decouple, and each nuclear contribution now evolves *adiabatically* according to the TDSE

$$\left[\sum_\nu^{N_n} \frac{-\hbar^2}{2M_\nu}\nabla_\nu^2 + \varepsilon_{BO}^{(k)}(\mathbf{R})\right]\chi_k(\mathbf{R},t) = i\hbar\partial_t\chi_k(\mathbf{R},t)\,, \tag{20}$$

under the effect of a potential produced only by the electrons in the adiabatic state k. This is the essence of the BO approximation. Analogously, in the limit of infinite nuclear masses, Eqs. (11) and (12) (Scherrer et al (2015); Schild et al (2016); Eich and Agostini (2016); Scherrer et al (2017)) reduce to the fundamental equations of the BO approximation, namely the static electronic equation (3) and a nuclear evolution equation identical to Eq. (20) with $\chi_k(\mathbf{R},t)$ replaced by the nuclear wavefunction $\chi(\mathbf{R},t)$ of the Exact Factorization.

If the nonadiabatic couplings cannot be neglected, the fully coupled electron-nuclear problem, summarized in Eq. (7) or Eqs. (11) and (12), has to be solved.

Electronic dynamics is simulated at a quantum-mechanical level employing quantum-chemistry approaches, either based on the electronic wavefunction or on the electronic density. If either the adiabatic or the diabatic basis are used to characterize the electronic subsystem, electronic dynamics is implied in the time evolution of the expansion coefficients (see for instance Eqs. (4) or (16)), since the basis functions are time-independent. On the other hand, (real-time) TDDFT yields an explicit evolution of the electronic subsystem, as the electrons are represented via their time-dependent one-body density. As we will show below, real-time TDDFT can be combined with a mean-field solution of the coupled electron-nuclear dynamics. The LR formulation of TDDFT, instead, is able to provide information about the time-independent electronic properties, such as adiabatic forces and nonadiabatic couplings, needed for approaches based on the Born-Huang expansion. Possible extensions of TDDFT to solve the electronic equation of the Exact Factorization are currently under investigation (Requist and Gross (2016)). Section 3 is devoted to a thorough review of the basis of TDDFT and of LR-TDDFT

Nuclear dynamics can be treated exactly or approximated at different levels, depending on the complexity of the system of interest. Simulation methods that retain the quantum character of nuclear dynamics are indeed very expensive, as the numerical cost for solving the quantum-mechanical problem scales exponentially with the number of degrees of freedom. Therefore, different strategies have been proposed over the years to make the problem numerically tractable. Quantum wavepacket propagation techniques aim at solving Eq. (7) either on grids (Lauvergnat and Nauts (2010, 2014); Sadri et al (2012)), or by expanding the nuclear wavepackets $\chi_k(\mathbf{R},t)$ on a basis where calculations are computationally cheaper (Meyer et al (1990); Burghardt et al (1999); Wang and Thoss (2003); Meyer and Worth (2003); Sadri et al (2014)). The major bottleneck of these approaches is the "pre-calculation" of the electronic properties, i.e., BO PESs and of the nonadiabatic couplings, needed to solve the nuclear equations. Attempts at solving exactly the coupled equations at the basis of the Exact Factorization are currently under investigations. On-the-fly calculations of electronic properties are instead possible, if only local nuclear information is necessary to solve (in an approximate way) Eq. (7). Full and ab initio multiple spawning methods (Martínez et al (1996); Martínez and Levine (1997); Ben-Nun and Martínez (1998); Ben-Nun et al (2000); Hack et al (2001); Ben-Nun and Martínez (2002); Virshup et al (2008)), similarly to direct-dynamics techniques (Worth et al (2004); Lasorne et al (2006, 2007); Worth et al (2008); Mendive-Tapia et al (2012); Richings et al (2015)), employ a representation of the nuclear wavepackets in terms of moving Gaussian functions, that evolve along trajectories determined either variationally or classically. Trajectory-based quantum-classical schemes adopt a representation of nuclear dynamics in terms of purely classical trajectories, as in the Ehrenfest and surface-hopping methods. They are indeed numerically cheaper than the methods above, but the price to pay is sometimes the neglect of important quantum-mechanical features both in the nuclear dynamics and in the coupling between electronic and nuclear motion. Similarly to direct dynamics and full multiple spawning, evolving the nuclei along trajectories enables us to exploit the locality of classical dynamics for on-the-fly simulations, where electronic infor-

mation is needed, and thus computed, only for the visited nuclear configurations. Trajectory-based solutions of Eqs. (11) and (12) have been proposed (Agostini et al (2014); Abedi et al (2014)), and the most recent developments (Min et al (2017)) will be reviewed in Section 4, along with Ehrenfest dynamics (Tully (1998)), trajectory surface hopping (Tully (1990); Doltsinis and Marx (2002); Böckmann et al (2010); Jasper et al (2004, 2006); Subotnik et al (2013); Curchod and Tavernelli (2013b); Jaeger et al (2012); Fang and Hammes-Schiffer (1999); Tapavicza et al (2007a); Craig et al (2005); Akimov and Prezhdo (2014)) and full/ab-initio multiple spawning (Martínez et al (1996); Martínez and Levine (1997); Ben-Nun and Martínez (1998); Ben-Nun et al (2000); Hack et al (2001); Ben-Nun and Martínez (2002); Virshup et al (2008)).

3 Electronic dynamics: Time-dependent density functional theory

3.1 Time-dependent density functional theory

The Hohenberg-Kohn (HK) theorem (Hohenberg and Kohn (1964)) of ground-state DFT states that knowledge of the ground-state density uniquely determines the external potential of the system (up to within a trivial constant) and thus the entire electronic Hamiltonian and the associated total ground-state energy. It is important to realize that ground-state DFT in nearly all applications is intimately tied to the BO approximation: the electronic density one calculates is the one produced by *clamped* nuclei. Then, by varying the positions of the clamped nuclei, ground-state DFT provides an efficient approach to map out the lowest BO PES and to calculate physical observables associated with the lowest BO PES, such as vibrational spectra, cohesive energies, barrier heights, etc. Higher BO PESs and the time evolution of systems strongly driven by external fields are not accessible wit ground-state DFT.

In their seminal paper, Runge and Gross (Runge and Gross (1984)) proved a theorem that established a 1-1 correspondence between the time-dependent density and the time-dependent external potential for systems evolving from a given initial many-electron state, Φ_0. The time evolution of the many-electron wavefunction is governed by the time-dependent Schrödinger equation

$$\begin{aligned} \hat{H}_{el}(t)\Phi(\mathbf{r},t) &= i\hbar\frac{\partial}{\partial t}\Phi(\mathbf{r},t) \\ \Phi(\mathbf{r},t_0) &= \Phi_0(\mathbf{r}) \end{aligned} \tag{21}$$

with Hamiltonian

$$\hat{H}_{el}(t) = \hat{T}_e(\mathbf{r}) + V_{ee}(\mathbf{r}) + v_{ext}(\mathbf{r},t)\,. \tag{22}$$

The general time-dependent external potential appearing in (22) covers different scenarios: one important case is the (short-time) electron dynamics with clamped nuclei, driven by an applied laser field

$$v_{ext}(\mathbf{r},t) = V_{nn}(\mathbf{R}) + V_{en}(\mathbf{r},\mathbf{R}) + \delta v_{app}(\mathbf{r},t). \tag{23}$$

Another case is the time-dependent electric potential produced by classically propagated point-like nuclei

$$v_{ext}(\mathbf{r},t) = V_{nn}(\mathbf{R}(t)) + V_{en}(\mathbf{r},\mathbf{R}(t)). \tag{24}$$

In complete detail, the Runge-Gross theorem ensures that the densities $\rho(\mathbf{r},t)$ and $\rho'(\mathbf{r},t)$ evolving from a common initial many-body state $\Phi_0 = \Phi(t_0)$ under the influence of two potentials $V_{ext}(\mathbf{r},t)$ and $V'_{ext}(\mathbf{r},t)$ will become different infinitesimally later than t_0 if the potentials are Taylor expandable around the initial time t_0 and differ by more than a purely time-dependent constant $V_{ext}(\mathbf{r},t) \neq V'_{ext}(\mathbf{r},t) + C(t)$. This implies that the potentials-to-densities map can be inverted:

$$\rho(\mathbf{r},t) \to v_{ext}[\rho](\mathbf{r},t). \tag{25}$$

The Runge-Gross proof does not depend on the particular form of the particle-particle interaction. The proof is valid for essentially any interaction, in particular also for no interaction. This establishes the map for non-interacting particles

$$\rho(\mathbf{r},t) \to v_s[\rho](\mathbf{r},t). \tag{26}$$

implying that the potential $v_s(\mathbf{r},t)$, which reproduces the interacting density, $\rho(\mathbf{r},t)$, in a non-interacting system is uniquely defined. From now on, this unique potential $v_s[\rho](\mathbf{r},t)$ will be called the *time-dependent Kohn-Sham potential*. The corresponding system of single-particle time-dependent Schrödinger equations

$$i\hbar\frac{\partial}{\partial t}\phi_k(\mathbf{r},t) = \left(-\frac{1}{2}\nabla^2 + v_s(\mathbf{r},t)\right)\phi_k(\mathbf{r},t), \quad k = 1,\ldots,N, \tag{27}$$

whose orbitals reproduce the interacting density via

$$\rho(\mathbf{r},t) = \sum_{i=1}^{N} |\phi_k(\mathbf{r},t)|^2 \tag{28}$$

are called *time-dependent Kohn-Sham (TDKS) equations*.

The Runge-Gross theorem guarantees uniqueness of the potentials $v_{ext}[\rho,\Phi_0](\mathbf{r},t)$ and $v_s[\rho,\{\phi_k^{(0)}(\mathbf{r})\}]$ for given initial many-body state Φ_0 and given initial orbitals $\{\phi_k^{(0)}(\mathbf{r})\}$, respectively (Gross and Kohn (1990)). Apart from uniqueness, whether or not, for a given function $\rho(\mathbf{r},t)$, the potential $v_{ext}(\mathbf{r},t)$ and $v_s(\mathbf{r},t)$ actually exist, is a separate question, known as (interacting and non-interacting) v-representability problem. This problem has been solved – once and for all – by van Leeuwen(van

Leeuwen (1999)), who demonstrated under mild conditions to be satisfied by the densities $\rho(\mathbf{r},t)$ that the potentials $v_{ext}(\mathbf{r},t)$ and $v_s(\mathbf{r},t)$ can be constructed explicitly as solutions of the Sturm-Liouville problem. Since this is a constructive proof, the solution of the TDDFT v-representability problem is much more satisfactory than the status of the v-representability problem in ground-state DFT where a complete characterization of the domains of the $v^{gs}_{ext}(\mathbf{r},t)$ and $v^{gs}_{s}(\mathbf{r},t)$ is still lacking.

The TDKS potential in Eq. (27) is usually written in the following form

$$v_s(\mathbf{r},t) = v_0(\mathbf{r},t) + v_H[\rho](\mathbf{r},t) + v_{xc}[\rho](\mathbf{r},t) \tag{29}$$

where $v_0(\mathbf{r},t)$ is the given external potential of the system at hand, $v_H[\rho](\mathbf{r},t)$ is the time-dependent Hartree potential

$$v_H[\rho](\mathbf{r},t) = \int d\mathbf{r}' \, \frac{\rho(\mathbf{r}',t)}{|\mathbf{r}-\mathbf{r}'|} \tag{30}$$

and $v_{xc}[\rho](\mathbf{r},t)$ is the universal exchange-correlation (*xc*) functional of TDDFT

$$v_{xc}[\rho](\mathbf{r},t) := v_s[\rho](\mathbf{r},t) - v_{ext}[\rho](\mathbf{r},t) - v_H[\rho](\mathbf{r},t). \tag{31}$$

The *xc* functional is well-defined through the right-hand side of Eq. (31): Uniqueness of $v_s[\rho]$ and $v_{ext}[\rho]$ is guaranteed by the Runge-Gross theorem and the existence over a well-characterized domain is covered by the van Leeuwen theorem. Formally, in addition to dependence on the density $\rho(\mathbf{r},t)$, the *xc* potential also depends on the initial many-body state Φ_0 and on the initial orbitals $\{\phi^{(0)}_k(\mathbf{r})\}$. If the initial state is a ground state, both Φ_0 and $\{\phi^{(0)}_k(\mathbf{r})\}$ are functionals of the initial ground-state density $\rho^{gs}_0(\mathbf{r},t)$ via the HK theorem and then the time-dependent *xc* potential becomes a functional of the time-dependent density alone. The density dependence of the exact time-dependent *xc* functional $v_{xc}[\rho(\mathbf{r}',t')](\mathbf{r},t)$ is non-local both in space and in time, i.e., the potential $v_{xc}(\mathbf{r},t)$ at point $\mathbf{r}$ and time t depends on the density values at all points $\mathbf{r}'$ and at all previous times $t' \leq t$.

An important aspect of the ground-state DFT is the HK variational principle which ensures that the total energy as functional of the density is minimized by the true ground-state density of the system at hand, and the value of the functional at the minimum is the true ground-state energy. The HK variational principle is important in two respects: first of all, the total energy is a quantity of prime interest and the variational principle guarantees that the lowest possible value is achieved. Of equal importance is the fact that the variational principle usually implies numerical stability of the iterative algorithms, such as the Kohn-Sham (KS) self-consistency cycle, because they ultimately go "downhill" in the total energy functional.

In the time-dependent case, variational principles play a less important role. First of all, the usual Frenkel variational principle of quantum mechanics

$$\delta \int_{t_0}^{t_1} dt \, \langle \Phi(t)| \, i\hbar \frac{\partial}{\partial t} - \hat{H} \, |\Phi(t)\rangle = 0 \tag{32}$$

normally does not have a minimum at the solution of the time-dependent Schrödinger equation. There is only a stationary point and consequently there is not guarantee of the stability of the associated time propagation algorithms. Moreover, unlike the ground-state energy, the value of functional (32) in the stationary point is zero and of no physical significance. Nevertheless, a TDDFT variational principle might still be desirable for some purposes, e.g., for the optimization of constrained densities.

Straightforward combination of the Runge-Gross map with the Frenkel variational principle (32) leads to a variational formulation of TDDFT (Runge and Gross (1984)) which was later found to give rise to serious inconsistencies (Gross et al (1994)). In particular, a non-causal *xc* kernel is found. This so-called causality paradox arises from the fact that arbitrary density variations lead to variations of the wavefunction at the upper boundary t_1 of the Frenkel integral (32). If the variations of the wavefunction are explicitly included, the causality paradox disappears (Vignale (2008)). Another way of the getting rid of the upper boundary t_1 of the Frenkel integral (32) is to formulate the TDDFT variational principle on the Keldysh contour which maps the final time back to the initial time. This formulation of the TDDFT variational principle was achieved by van Leeuwen (van Leeuwen (1998)).

3.2 Linear-response TDDFT

Many applications of TDDFT deal with weak probes of the ground state of a static potential $v_0(\mathbf{r})$, mediated by a small time-dependent perturbation $\delta v_{app}(\mathbf{r},t)$. The goal of linear-response TDDFT is to calculate the induced first-order change $\delta\rho(\mathbf{r},t)$ in the density (Gross et al (1996)). To this end we look at the density $\rho[v_{ext}](\mathbf{r},t)$ as functional of the external potential and perform a functional Taylor expansion at the unperturbed ground-state potential $v_0(\mathbf{r},t)$

$$\rho[v_{ext}](\mathbf{r},t) = \rho\left[v_0+\delta v_{app}\right](\mathbf{r},t) \tag{33}$$

$$= \rho[v_0](\mathbf{r}) + \int d\mathbf{r}' \int dt' \left.\frac{\delta\rho(\mathbf{r},t)}{\delta v_{ext}(\mathbf{r}',t')}\right|_{v_0} \delta v_{app}(\mathbf{r}',t') + \ldots . \tag{34}$$

The functional derivative on the right-hand side of Eq. (34), which connects the change in the density with the perturbation is of enormous physical significance. It is known as *density-density response function* and will henceforth be denoted by $\chi(\mathbf{r},t,\mathbf{r}',t')$:

$$\chi(\mathbf{r},t,\mathbf{r}',t') = \left.\frac{\delta\rho(\mathbf{r},t)}{\delta v_{ext}(\mathbf{r}',t')}\right|_{v_0} . \tag{35}$$

The associated change in the density is known as *linear density response*

$$\delta\rho(\mathbf{r},t) = \int d\mathbf{r}' \int dt' \, \chi(\mathbf{r},t,\mathbf{r}',t')\delta v_{app}(\mathbf{r}',t'). \tag{36}$$

Since $\chi(\mathbf{r},t,\mathbf{r}',t')$ only depends on $t-t'$, Eq. (36) is usually Fourier-transformed to the frequency domain

$$\delta\rho(\mathbf{r},\omega) = \int d\mathbf{r}' \, \chi(\mathbf{r},\mathbf{r}',\omega)\delta v_{app}(\mathbf{r}',\omega) \tag{37}$$

where, for simplicity, we use the same symbol for a function and for its Fourier transform. The poles of $\chi(\mathbf{r},\mathbf{r}',\omega)$ provide the charge-neutral excitation energies of the unperturbed many-body system.

One may also look at the density $\rho_s[v_s](\mathbf{r},t)$ of non-interacting particles and their density-density response function

$$\chi_s(\mathbf{r},t,\mathbf{r}',t') = \left.\frac{\delta\rho_s(\mathbf{r},t)}{\delta v_s(\mathbf{r}',t')}\right|_{v_{s,0}}. \tag{38}$$

While the full interacting density-density response function (35) is very hard to evaluate (in many-body language it is the reducible polarization propagator of the interacting system), the non-interacting counterpart is relatively easy to calculate: Its Fourier transform reads

$$\chi_s(\mathbf{r},\mathbf{r}',\omega) = \sum_{ij\sigma,kl\tau} \phi_{i\sigma}(\mathbf{r})\phi^*_{j\sigma}(\mathbf{r})\phi_{k\tau}(\mathbf{r}')\phi^*_{l\tau}(\mathbf{r}')\chi^{\mathrm{s}}_{ij\sigma,kl\tau}(\omega)\,. \tag{39}$$

with

$$\chi^{\mathrm{s}}_{ij\sigma,kl\tau}(\omega) = \delta_{\sigma,\tau}\delta_{i,k}\delta_{j,l}\frac{f_{j\sigma}-f_{i\sigma}}{\omega-(\varepsilon_{i\sigma}-\varepsilon_{j\sigma})}, \tag{40}$$

where $\varepsilon_{i\sigma}$ are the ground-state KS orbital energies and $f_{i\sigma}$ their occupations in the ground state. Multiplying this equation – in the operator sense – from the left with χ_s and from the right with χ, and performing a Fourier transform to frequency space, one obtains the following Dyson-like equation for the response function (Petersilka et al (1996))

$$\chi(\omega) = \chi^s(\omega) + \chi^s(\omega) * f_{Hxc}(\omega) * \chi(\omega)\,. \tag{41}$$

This equation constitutes the cornerstone of linear-response TDDFT.

Acting with the operator in equation (41) on an arbitrary perturbation $\delta v_{app}(\mathbf{r},\omega)$ and using the definition (37) of the linear density response, one ends up with an integral equation for the desired density response

$$\delta\rho(\omega) = \chi_s(\omega) * (\delta v_{app}(\omega) + f_{Hxc}(\omega) * \delta\rho(\omega))\,. \tag{42}$$

An iterative numerical solution of this equation yields the full linear density response as function of ω and was first achieved by Zangwill and Soven (Zangwill and Soven (1980)) for atoms in the frequency regime above the continuum threshold. If one is interested in the discrete spectrum of the system, i.e., the discrete poles

of the linear density response, a considerable simplification can be achieved (Gross and Kohn (1985); Grabo et al (2000); Petersilka et al (1996); Jamorski et al (1996)), leading to a generalized eigenvalue equation

$$\begin{bmatrix} \mathbb{A} & \mathbb{B} \\ \mathbb{B}^* & \mathbb{A}^* \end{bmatrix} \begin{bmatrix} \mathbf{X}_n \\ \mathbf{Y}_n \end{bmatrix} = \omega_n \begin{bmatrix} \mathbb{I} & 0 \\ 0 & -\mathbb{I} \end{bmatrix} \begin{bmatrix} \mathbf{X}_n \\ \mathbf{Y}_n \end{bmatrix}. \tag{43}$$

where the matrices $\mathbb{A}(\omega)$ and $\mathbb{B}(\omega)$ are given by

$$A_{ia\sigma,jb\tau}(\omega) = \delta_{\sigma,\tau}\delta_{i,j}\delta_{a,b}(\varepsilon_{a\sigma} - \varepsilon_{i\sigma}) + K_{ia\sigma,jb\tau}(\omega) \tag{44}$$

$$B_{ia\sigma,jb\tau}(\omega) = K_{ia\sigma,bj\tau}(\omega). \tag{45}$$

The matrices $\mathbb{A}$ and $\mathbb{B}$ are frequency-independent within the *adiabatic approximation*, which approximate the exchange-correlation kernel f_{xc} has a frequency-independent term (Casida (2009)). (Note that memory-dependent functionals were proposed (Dobson et al (1997); Ullrich and Tokatly (2006); Wijewardane and Ullrich (2008); Kurzweil and Baer (2004)), even if not commonly used.) Solving the Casida equation provides excitation energies and oscillator strengths for a molecular system.

A common approximation, the Tamm-Dancoff approximation (TDA), consists in neglecting the hole-particle terms, $\mathbf{Y}_n \equiv 0$, leading to the simpler eigenvalue equation (Hirata and Head-Gordon (1999)):

$$\mathbb{A}\mathbf{X}_n = \omega_n \mathbf{X}_n. \tag{46}$$

While the TDA allows for the design of better-converging algorithms (Hirata and Head-Gordon (1999); Hutter (2003)), it also sometimes leads to better results than the full Casida equation (Casida et al (2000); Tapavicza et al (2008a); Casida and Huix-Rotllant (2012)). This observation might find its source from the form of the Casida equation for pure density functional theory. The Casida equation involves the linear response of the one-body density matrix and therefore accommodate the response treatment of hybrid functions in a natural way. However, when functionals with no Hartree-Fock contribution are considered, the matrix $(\mathbb{A} - \mathbb{B})$ becomes diagonal (see footnote [1] below). Then, the exact secular equation takes a similar form as within the TDA, with $\mathbb{A}$ corrected by a contribution from $\mathbb{B}$ (Casida (2009)) and relates to the exact equation derived from pure density functional response theory (Grabo et al (2000)). It is, however, important to note that within TDA the Thomas-Reiche-Kuhn sum rule is not fulfilled (Furche (2001); Hutter (2003)).

3.2.1 Pitfalls of the approximation of practical LR-TDDFT

LR-TDDFT has been successfully applied to compute excitation energies and properties for a large number of molecular systems (Stratmann et al (1998); Hirata and Head-Gordon (1999); Maitra et al (2003); Dreuw and Head-Gordon (2005); Ullrich (2012); Casida (2009); Elliott et al (2009); Casida and Huix-Rotllant (2012);

Adamo and Jacquemin (2013); Laurent and Jacquemin (2013)) However, while the LR-TDDFT formalism is *in principle* exact, its practical application to compute excitation energies for molecules require the use of a series of approximations of the *xc*-functional and its functional derivatives (like the adiabatic approximation), which can lead to dramatic failures (Ullrich (2012); Marques et al (2012); Casida (2009); Casida and Huix-Rotllant (2012)). As a result of the adiabatic approximation, LR-TDDFT is for example not able to properly describe electronic states with a dominant (>50%, see Ref. (Tozer and Handy (2000); Ullrich (2012))) double excitation character (Hsu et al (2001); Maitra et al (2004); Cave et al (2004); Levine et al (2006); Elliott et al (2011)). Also, the combination of an inaccurate description of derivative discontinuities, the problem of self-interaction error, the incorrect long-range properties of currently used *xc*-potentials, and the adiabatic approximation are all at the heart of the most critical issue of LR-TDDFT: the charge transfer failure (Dreuw et al (2003); Tozer (2003); Gritsenko and Baerends (2004); Dreuw and Head-Gordon (2004); Maitra (2005); Wiggins et al (2009); Hellgren and Gross (2012)). LR-TDDFT, within the adiabatic approximation and using standard functionals, suffers to describe charge transfer excitations, i.e., excitations between a donor and an acceptor that are spatially separated. Long-range corrected functionals Leininger et al (1997); Iikura et al (2001); Yanai et al (2004) can, however, strongly improve the situation. The adiabatic approximation also leads to difficulties in describing conical intersections between the ground and first electronic state (Levine et al (2006)), even if, at least in some cases, the use of the TDA improves the description of these critical points (Tapavicza et al (2008a); Marques et al (2012)).

3.3 Nonadiabatic coupling vectors and nuclear forces within LR-TDDFT

The Casida equation introduced above gives a direct access to excitation energies and oscillator strength. Nonadiabatic dynamics will require additional quantities like nonadiabatic coupling vectors (last electronic term in Eq. (8)) or excited-state nuclear forces. In the following, we will describe a strategy to compute matrix elements of one-body operator within a LR-TDDFT framework, using the concept of *auxiliary many-electron wavefunctions* that will give us access to nonadiabatic coupling vectors as well as other quantities.

3.3.1 Matrix elements in LR-TDDFT

Our goal is to find a general strategy for evaluating matrix elements of the form

$$\langle \varphi_{\mathbf{R}}^{(0)} | \hat{\mathscr{O}} | \varphi_{\mathbf{R}}^{(n)} \rangle \tag{47}$$

within LR-TDDFT, where the states $|\varphi_{\mathbf{R}}^{(0)}\rangle$ and $|\varphi_{\mathbf{R}}^{(n)}\rangle$ describe the ground state and n^{th} electronic excited state wavefunctions, respectively. To achieve this goal, we will proceed by a direct comparison with the same quantity derived using many-body perturbation theory (MBPT). Therefore, we start with a short outline of the main linear-response equations in MBPT.

From the definition of the retarded density-density response function

$$\chi(\mathbf{r},t,\mathbf{r}',t') = \Pi^R(\mathbf{r},t,\mathbf{r}',t') = -i\theta(t-t')\frac{\langle\varphi_{\mathbf{R}}^{(0)}|[\hat{\rho}(\mathbf{r},t),\hat{\rho}(\mathbf{r}',t')]|\varphi_{\mathbf{R}}^{(0)}\rangle}{\langle\varphi_{\mathbf{R}}^{(0)}|\varphi_{\mathbf{R}}^{(0)}\rangle}, \quad (48)$$

the change of an observable $\mathscr{O}$, under the influence of a perturbation $v_{ext}(\mathbf{r}',t')$ in the linear-response regime is given by

$$\delta\mathscr{O}(t) = \int_0^\infty dt' \int d\mathbf{r} \int d\mathbf{r}'\, o(\mathbf{r}) v_{ext}(\mathbf{r}',t')\chi(\mathbf{r},t,\mathbf{r}',t') \quad (49)$$

(here we consider an interaction of the form $\delta v^{ext}(\mathbf{r}',t') = v'(\mathbf{r}')E(t')$). If χ depends only on the difference $(t-t')$, the Fourier transform in time gives

$$\delta\mathscr{O}(\omega) = \int d\mathbf{r} \int d\mathbf{r}'\, o(\mathbf{r}) v'(\mathbf{r}') E(\omega)\chi(\mathbf{r},\mathbf{r}',\omega)\,. \quad (50)$$

This expression can be rewritten, after a bit of algebra (Curchod et al (2013)), as a sum-over-states (SOS) formula

$$\delta\mathscr{O}(\omega) = -2\sum_n \frac{\omega_n \langle\varphi_{\mathbf{R}}^{(0)}|\hat{\mathscr{O}}|\varphi_{\mathbf{R}}^{(n)}\rangle\langle\varphi_{\mathbf{R}}^{(n)}|\hat{v}'E(\omega)|\varphi_{\mathbf{R}}^{(0)}\rangle}{\omega_n^2-\omega^2}\,, \quad (51)$$

where $|\varphi_{\mathbf{R}}^{(n)}\rangle$ and ω_n are the true excitation energies and wavefunctions.

Meanwhile, if we use the KS representation of LR-TDDFT as above, the change of observable is in matrix representation

$$\delta\mathscr{O}(\omega) = \sum_{ij\sigma,kl\tau} o_{ij\sigma}\chi_{ij\sigma,kl\tau}(\omega)v'_{kl\tau}E(\omega)\,, \quad (52)$$

where $o_{ij\sigma} = \langle\phi_{i\sigma}|\mathscr{O}(\omega)|\phi_{j\sigma}\rangle$ and $v'_{kl\tau} = \langle\phi_{l\tau}|v'(\mathbf{r})|\phi_{k\tau}\rangle$. Similarly, a SOS formula can also be derived for LR-TDDFT (see Refs. (Curchod et al (2013)) for a derivation), and reads

$$\delta\mathscr{O}(\omega) = -2\sum_n \mathbf{o}^\dagger \frac{(\mathbb{A}-\mathbb{B})^{1/2}\mathbf{Z}_n\mathbf{Z}_n^\dagger(\mathbb{A}-\mathbb{B})^{1/2}}{\omega_n^2-\omega^2}\mathbf{v}'E(\omega)\,. \quad (53)$$

with $\mathbf{Z}_n$ is related to the eigenvectors of Eq. (43) according to (Casida (2009)) $\mathbf{Z}_n = (\mathbb{A}-\mathbb{B})^{-1/2}(\mathbf{X}_n+\mathbf{Y}_n)$.

Comparing the residues of LR-TDDFT response function Eq. (53) with the residues of the MBPT response function Eq. (51) at equal energy ω_n, we obtain

the following identity [1]

$$\langle \varphi_{\mathbf{R}}^{(0)} | \hat{\mathscr{O}} | \varphi_{\mathbf{R}}^{(n)} \rangle = \sum_{ij\sigma}^{(f_{i\sigma}-f_{j\sigma})>0} \frac{1}{\sqrt{\omega_n}} o_{ij\sigma} \left((\mathbb{A}-\mathbb{B})^{1/2} \mathbf{Z}_n \right)_{ij\sigma} . \tag{54}$$

This equation was derived by Casida (Casida (1995)) and then applied by Tavernelli et al. and Hu et al. for the calculation of the nonadiabatic coupling vectors between the ground state and an excited state. A similar equation was also given in Ref. (Chernyak and Mukamel (1996)).

3.3.2 The concept of auxiliary many-electron wavefunction

It may be useful at this point to investigate the possibility to further simplify the definition and the calculation of matrix elements within LR-TDDFT by means of the definition of a set of "auxiliary" multideterminantal many-electron wavefunctions based on KS orbitals. This route was first explored by Casida (Casida (1995)) to solve the assignment problem of the LR-TDDFT excited state transitions and then further developed by Tavernelli et. al (Tapavicza et al (2007b)) in relation to the calculation of matrix elements in the linear and second-order response regimes (Tavernelli et al (2009b,a, 2010)).

In Ref. (Tavernelli et al (2009a)), we showed that defining the ground state many-electron wavefunction $\langle \mathbf{r}_1, \mathbf{r}_2, \mathbf{r}_3, \ldots, \mathbf{r}_{N_{el}} | \tilde{\varphi}_{\mathbf{R}}^{(0)} \rangle$ as a Slater determinant of all occupied KS orbitals $\{\phi_i\}_{i=1}^{N_{el}}$ and the excited state wavefunction corresponding to the excitation energy ω_n as

$$\begin{aligned} \langle \mathbf{r}_1, \mathbf{r}_2, \mathbf{r}_3, \ldots, \mathbf{r}_{N_{el}} | \tilde{\varphi}_{\mathbf{R}}^{(n)} \rangle &= \sum_{ia\sigma} \sqrt{\frac{\varepsilon_a - \varepsilon_i}{\omega_n}} (\mathbf{Z}_n)_{ia\sigma} \hat{a}_{a\sigma}^{\dagger} \hat{a}_{i\sigma} \langle \mathbf{r}_1, \mathbf{r}_2, \mathbf{r}_3, \ldots, \mathbf{r}_{N_{el}} | \tilde{\varphi}_{\mathbf{R}}^{(0)} \rangle \\ &= \sum_{ia\sigma} \mathscr{C}_{ia\sigma}^{n} \langle \mathbf{r}_1, \mathbf{r}_2, \mathbf{r}_3, \ldots, \mathbf{r}_{N_{el}} | \tilde{\varphi}_{\mathbf{R},i\sigma}^{a\sigma} \rangle, \end{aligned} \tag{55}$$

we obtain for any one-body operator of the form $\hat{\mathscr{O}} = \sum_{pq\sigma} o_{pq\sigma} \hat{a}_{p\sigma}^{\dagger} \hat{a}_{q\sigma}$ (where p, q are general indices) the correct linear-response expression for the matrix element $\langle \varphi_{\mathbf{R}}^{(0)} | \hat{\mathscr{O}} | \varphi_{\mathbf{R}}^{(n)} \rangle$. Eq. (55) is derived from Eq. (54) where now the index i runs over all occupied and a over the unoccupied (virtual) KS orbitals and $|\tilde{\varphi}_{\mathbf{R},i\sigma}^{a\sigma}\rangle$ denotes a singly-excited Slater determinant defined by the transition $i\sigma \rightarrow a\sigma$. This theory was then successfully extended to the case of the calculation of matrix elements between two excited state wavefunctions, $\langle \varphi_{\mathbf{R}}^{(n)} | \hat{\mathscr{O}} | \varphi_{\mathbf{R}}^{(m)} \rangle$ as will be briefly discussed in the next section on the calculation of nonadiabatic coupling vectors.

[1] As stated before, with no Hartree-Fock exchange contribution in the functional, $(\mathbb{A}-\mathbb{B})$ is diagonal and becomes (Casida (2009)):

$$(\mathbb{A}-\mathbb{B})_{ia\sigma,jb\tau} = \delta_{i,j}\delta_{a,b}\delta_{\sigma,\tau}(\varepsilon_{a\tau} - \varepsilon_{i\tau}) .$$

It is important to further stress the fact that both auxiliary functions introduced above have a physical meaning only when used within LR-TDDFT for the calculation of matrix elements of the type $\langle\tilde{\varphi}^{(0)}_{\mathbf{R}}|\hat{\mathscr{O}}|\tilde{\varphi}^{(n)}_{\mathbf{R}}\rangle$ and eventually $\langle\tilde{\varphi}^{(n)}_{\mathbf{R}}|\hat{\mathscr{O}}|\tilde{\varphi}^{(m)}_{\mathbf{R}}\rangle$. The use of this representations of the ground state and excited state KS many-electron wavefunctions in other contexts is not justified.

3.3.3 Nonadiabatic coupling vectors within LR-TDDFT

Using the concept of the auxiliary many-electron wavefunction approach described above, we can now propose an approach for the calculation of nonadiabatic vectors within LR-TDDFT.

Couplings between ground and excited states

We start from an alternative definition of the NACV (Epstein (1954)) (see also Ch. 5 of Ref. (Baer (2006)) for a complete discussion) between the ground (0) state and the n^{th} excited state for a molecular system characterized by nuclear coordinates $\mathbf{R}$ in the configuration space ($\mathbb{R}^{3N_n}$)

$$\mathbf{d}^{\gamma}_{0n} = \frac{\langle\varphi^{(0)}_{\mathbf{R}}|\partial_{\gamma}\hat{H}_{BO}|\varphi^{(n)}_{\mathbf{R}}\rangle}{\varepsilon^{(n)}_{BO}(\mathbf{R}) - \varepsilon^{(0)}_{BO}(\mathbf{R})} \tag{56}$$

where γ is an atomic label, $\hat{H}_{BO}$ is the electronic Hamiltonian, and $\partial_{\gamma}\hat{H}_{BO} = \partial\hat{H}_{BO}/\partial\mathbf{R}_{\gamma}$.

Applying the results of the above sections on the evaluation of matrix elements of the form $\langle\varphi^{(0)}_{\mathbf{R}}|\hat{\mathscr{O}}|\varphi^{(n)}_{\mathbf{R}}\rangle$ in LR-TDDFT to the NACV gives directly the desired expression

$$\mathbf{d}^{\gamma}_{0n} = \sum_{ij\sigma}^{(f_{i\sigma}-f_{j\sigma})>0} \frac{1}{(\omega_n)^{3/2}} h^{\gamma}_{ij\sigma} \left((\mathbb{A}-\mathbb{B})^{1/2}\mathbf{Z}_n\right)_{ij\sigma} \tag{57}$$

where $h^{\gamma}_{ij\sigma} = \int d\mathbf{r}\, \partial_{\gamma}\hat{H}_{BO}\, \phi^{*}_{i\sigma}(\mathbf{r})\phi_{j\sigma}(\mathbf{r})$.

This formula for the NACVs within LR-TDDFT was derived several times in the literature using slightly different formalisms. The first derivation was given by Chernyak and Mukamel (Chernyak and Mukamel (2000)) using a classical Liouville dynamics for the single-electron density matrix, followed by Baer (Baer (2002)). Later, Tavernelli et al. (Tapavicza et al (2007b); Tavernelli et al (2009b)) and Hu et al. (Hu et al (2007, 2008)) arrived to the same result (Eq. (57)) using the most widely used formulation based on Casida's LR-TDDFT equations (Casida (1995)).

Concerning the numerical implementation of Eq. (56) several approaches have also been proposed that differ mainly in the choice of the basis set and in the way the implicit dependence of the pseudopotentials on the nuclear positions is treated. Due to the technical nature of this subject, we will not go through the numerical

details but better refer to the literature, which is very rich on this subject (Tavernelli et al (2009b); Hu et al (2007); Send and Furche (2010); Hu et al (2010, 2012)).

Couplings between excited states

LR-TDDFT only gives access strictly speaking to the couplings between ground and excited state. However, the concept of LR-TDDFT auxiliary many-electron wavefunctions can also be used as a good approximation, exact within the Tamm-Dancoff approximation, to compute couplings between excited states (Tavernelli et al (2010)), $\mathbf{d}_{kn}$. An exact derivation of these coupling terms *beyond* the linear response formalism of TDDFT was also proposed in the literature (Li and Liu (2014); Li et al (2014); Ou et al (2015)). However, this formalism implies the calculation of an exchange-correlation hyperkernel and leads to the critical appearance of divergences in the couplings as a result of the adiabatic approximations (Parker et al (2016)).

3.4 Nuclear forces within LR-TDDFT

Excited-state dynamics using LR-TDDFT will also require the calculation of nuclear forces. Among the different approaches developed for the calculation of analytic derivatives, the Lagrangian method (Helgaker and Jørgensen (1989)) is of particular interest because of its numerical efficiency. However, the derivation of LR-TDDFT forces is technically involved and goes beyond the scope of this Chapter. We refer the interested reader to the abundant literature on the subject (Pulay (1987); Hutter (2003); Deglmann et al (2002); Rappoport and Furche (2005); Marx and Hutter (2009)).

4 Nuclear dynamics: Trajectory-based quantum-classical dynamics

In this section, different approaches to nonadiabatic electron-nuclear dynamics will be presented, namely the Ehrenfest scheme (Tully (1998)), surface hopping (Tully (1990)), the coupled-trajectory mixed quantum-classical (CT-MQC) method derived from the Exact Factorization (Min et al (2015)), and full multiple spawning (Martínez et al (1996)). Their common feature is the use of trajectories to explore the nuclear configuration space, which are subject to the time-dependent effect of the electrons in the ground state as well as in the excited states. The electronic properties needed in the calculations can be determined on-the-fly based on ab initio electronic structure methods. For the purpose of this work, TDDFT and its LR formulation will be employed. Other approaches based on Bohmian trajectories are

also possible (Curchod et al (2011); Curchod and Tavernelli (2013a); Tavernelli (2013)) but they will not be discussed in this book chapter.

Ehrenfest, surface hopping and CT-MQC are based on a purely classical description of nuclear motion, that is coupled to the quantum-mechanical evolution of the electrons. In the three approaches, a hypothesis is made to decompose the full TDSE into two coupled equations, one describing the evolution of the electronic subsystem, and the other describing the evolution of the nuclear subsystem. The main difference among them lies in the procedure followed for such decomposition. In particular, only the Exact Factorization starts from an Ansatz for the molecular wavefunction, which translates into exact coupled electronic and nuclear equations. Only in a second step, the nuclear evolution is modelled using classical trajectories. The full multiple spawning scheme, on the other hand, introduces an expansion in terms of Gaussian wavepackets to represent each nuclear coefficients $\chi_k(\mathbf{R},t)$ of the Born-Huang expansion (4). The parameters of the Gaussians are evolved classically, under the assumption that classical dynamics samples correctly the nuclear configuration space. Indeed, in the limit of an infinite number of Gaussians, full multiple spawning converges to an exact description of the electron-nuclear problem.

4.1 Ehrenfest dynamics

To derive Ehrenfest decomposition, one makes the assumption that the full wavefunction can be written as a single product of a purely electronic $\Phi(\mathbf{r},t)$ and a purely nuclear $\chi(\mathbf{R},t)$ wavefunction,

$$\Psi(\mathbf{r},\mathbf{R},t) = e^{\frac{i}{\hbar}\int_0^t dt' E_{BO}(t')}\Phi(\mathbf{r},t)\chi(\mathbf{R},t)\,. \tag{58}$$

Here, the time-dependent phase on the right-hand side is inserted to simplify the following equations derived from such an Ansatz, thus the energy $E_{BO}(t)$ is chosen as

$$E_{BO}(t) = \int d\mathbf{r}\,\Phi^*(\mathbf{r},t) i\hbar\partial_t \Phi(\mathbf{r},t)\,. \tag{59}$$

The product form of the molecular wavefunction in Eq. (58) is clearly uncorrelated, and in this initial Ansatz lies the fundamental approximation of the Ehrenfest scheme. When Eq. (58) in inserted into the molecular TDSE (1), the coupled equations

$$\left[\hat{T}_e(\mathbf{r})+\hat{V}_{ee}(\mathbf{r})+\int d\mathbf{R}\,\chi^*(\mathbf{R},t)\left[\hat{V}_{nn}(\mathbf{R})+\hat{V}_{en}(\mathbf{r},\mathbf{R})\right]\chi(\mathbf{R},t)\right]\Phi(\mathbf{r},t)=i\hbar\partial_t\Phi(\mathbf{r},t) \tag{60}$$

$$\left[\sum_\nu\frac{-\hbar^2}{2M_\nu}\nabla_\nu^2+\int d\mathbf{r}\,\Phi^*(\mathbf{r},t)\hat{H}_{BO}(\mathbf{r},\mathbf{R})\Phi(\mathbf{r},t)\right]\chi(\mathbf{R},t)=i\hbar\partial_t\chi(\mathbf{R},t) \tag{61}$$

are derived, by averaging over the instantaneous nuclear, in Eq. (60), and electronic, in Eq. (61), state. In both equations, the wavefunctions $\Phi(\mathbf{r},t)$ and $\chi(\mathbf{R},t)$ are supposed to be normalized. Therefore, Eq. (60) describes the evolution of the electrons in the mean field created by the nuclei, whereas the nuclei move according to Eq. (61) in the mean field of the electrons.

A quantum-classical algorithm can be derived from Eqs. (60) and (61) by approximating classically the nuclear equation, that is by determining the force to propagate the nuclei as trajectories. A standard procedure can be followed, by introducing a complex-phase representation of $\chi(\mathbf{R},t)$, and by only considering terms $\mathscr{O}(\hbar^0)$ in the asymptotic expansion of the complex phase in powers of $\hbar$ (Van Vleck (1928)). The equation for the zeroth order term $S(\mathbf{R},t)$ of this expansion is thus obtained, namely

$$\partial_t S(\mathbf{R},t)=-\left[\sum_\nu\frac{[\nabla_\nu S(\mathbf{R},t)]^2}{2M_\nu}+\int d\mathbf{r}\,\Phi^*(\mathbf{r},t)\hat{H}_{BO}(\mathbf{r},\mathbf{R})\Phi(\mathbf{r},t)\right]. \tag{62}$$

This Hamilton-Jacobi-like equation can be solved via characteristics, thus yielding the expression of the classical (Ehrenfest) force as

$$\mathbf{F}_\nu(t)=-\nabla_\nu\int d\mathbf{r}\,\Phi^*(\mathbf{r},t)\hat{H}_{BO}(\mathbf{r},\mathbf{R})\Phi(\mathbf{r},t)\,. \tag{63}$$

The classical approximation is also introduced in the electronic evolution equation (60). Here, the nuclear density $|\chi(\mathbf{R},t)|^2$ is approximated as a product of δ-functions centered at each time at the position of the classical nuclei, that is at the position of the classical trajectory $\mathbf{R}^{(I)}(t)$. Therefore, the TDSE describing the evolution of $\Phi(\mathbf{r},t)$ becomes

$$\hat{H}_{BO}\left(\mathbf{r},\mathbf{R}^{(I)}(t)\right)\Phi\left(\mathbf{r},\mathbf{R}^{(I)}(t),t\right)=i\hbar\partial_t\Phi\left(\mathbf{r},\mathbf{R}^{(I)}(t),t\right). \tag{64}$$

The electronic wavefunction acquires an implicit dependence on the nuclear positions, expressed as the classical trajectory, via the dependence of the BO Hamiltonian on $\mathbf{R}^{(I)}(t)$. The trajectory I of the nucleus ν is determined by solving Newton's equation with force

$$\mathbf{F}_\nu^{(I)}(t)=\int d\mathbf{r}\,\Phi^*(\mathbf{r},\mathbf{R}^{(I)}(t),t)\left[-\nabla_\nu\hat{H}_{BO}(\mathbf{r},\mathbf{R}^{(I)}(t))\right]\Phi(\mathbf{r},\mathbf{R}^{(I)}(t),t)\,, \tag{65}$$

where now a label (I) has been introduced to show that along a trajectory, Eqs. (64) and (65) have to be evolved consistently. Multiple trajectories can also be employed, to "wash out" some of the details of the coherent evolution along a single trajectory. Nuclear and electronic observables can thus be determined as averages over this ensemble of trajectories.

As it provides the true time-dependent electronic density, TDDFT can be used within an Ehrenfest dynamics scheme to perform nonadiabatic molecular dynamics. The mapping of the nuclear equation (Eq. (65)) into the DFT formalism is straightforward and only requires the description of the forces $\langle -\nabla_\nu \hat{H}_{BO}(\mathbf{r}, \mathbf{R}^{(I)}(t))\rangle$ as a functional of the time-dependent density $\rho(\mathbf{r},t)$. If we replace the expectation value of the electronic Hamiltonian with the DFT energy evaluated with the exchange-correlation potential $v_{xc}[\rho]|_{\rho(\mathbf{r})\leftarrow\rho(\mathbf{r},t)}$, the gradient with respect to the nuclear coordinates can be performed analytically as in the case of the adiabatic BO dynamics and the Car-Parrinello (Car and Parrinello (1985)) molecular dynamics schemes (Marx and Hutter (2009)).

4.1.1 Application of Ehrenfest dynamics combined with TDDFT

As Ehrenfest dynamics gives a direct access to electronic dynamics, it is a method of choice to investigate the dynamics of the electronic density and subsequent nuclear dynamics after a strong perturbation. Such perturbation can be induced by the action of an external light pulse or through the collision with a highly-charged particle, generating either an electronic excitation or, in the some other cases, electron abstraction (Tavernelli et al (2005); Tavernelli (2006); Castro et al (2004); Li et al (2005); Yagi and Takatsuka (2005); Andrade et al (2009); Moss et al (2009); Liang et al (2010); Gaigeot et al (2010); Lopez-Tarifa et al (2011); Elliott and Maitra (2012); Tavernelli (2015)). The latter takes place when an XUV attosecond pulse interacts with a molecule and leads to a core ionization. In a Born-Huang picture, such an ultrafast ionization leads to the generation of an electronic wavepacket, i.e., the generation of a coherent superposition of different nuclear contributions on a large number of electronic states (the number of electronic states being considered depends on the bandwidth of the ionizing pulse). Ehrenfest dynamics combined with TDDFT offers an alternative to the Born-Huang picture by only requiring the generation of an initial electronic density to represent the initial ionized state. Martín et al. employed this strategy to study the role of nuclear motion in the electronic dynamics upon XUV ultrafast ionization of a small amino acid, glycine (Lara-Astiaso et al (2017)). The one-electron ionization generated by the sub-300-as XUV pulse generates an electronic wavepacket that can be described by a coherent superposition of more than ten one-hole states, in an energy domain ranging from 17 to 35 eV (the pulse bandwidth). The electronic density corresponding to this electronic wavepacket, $\rho(\mathbf{r},t_0)$, is used as initial condition for two simulations: (*i*) real-time TDDFT with frozen nuclei and (*ii*) real-time TDDFT combined with Ehrenfest dynamics. As a result of the nature of the electronic wavepacket, the time-evolution of the unpaired electron (with respect to the initial density) shows that the electron

migrates over the entire molecular scaffold with a dynamics that is characterized by only few, system dependent, frequencies (Fig. 1). This is the behavior that one would expect in the case the ionized electron is removed from one given localized orbital. Comparing the two panels of Fig. 1, we observe that nuclear motion starts altering the electronic dynamics already after the first 10 fs of dynamics, emphasizing the importance of including nuclear dynamics in such simulations. However, it is important to note that the mean-field character of Ehrenfest dynamics might hamper a more detailed study of the electronic wavepacket dynamics, in particular due to the underestimation of decoherence and dephasing effects at longer time scales (Vacher et al (2017)). The ease of the Ehrenfest formalism combined with the efficiency of TDDFT offer nevertheless a valid tool for the study of the short-time electronic wavepacket dynamics in molecular systems.

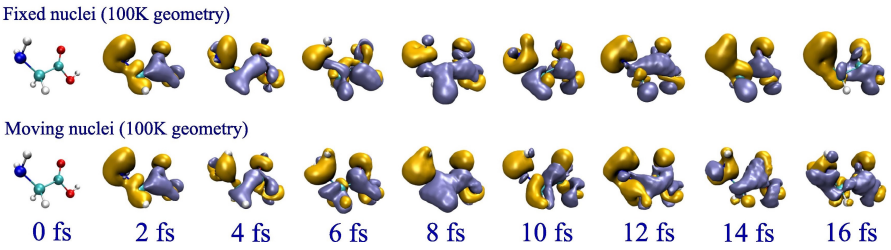

Fig. 1: Spin density differences at different times after interaction of a XUV attosecond pulse with the glycine molecule. The initial conditions correspond to a geometry obtained after thermalization at 100 K. Adapted from Chemical Physics Letters, 683, M. Lara-Astiaso, A. Palacios, P. Decleva, I. Tavernelli, F. Martín, Role of electron-nuclear coupled dynamics on charge migration induced by attosecond pulses in glycine, 357, Copyright (2017), with permission from Elsevier.

4.2 Surface hopping

Surface-hopping decomposition is derived under the preliminary assumption that the nuclei evolve along classical trajectories. Therefore, the BO Hamiltonian acquires an implicit time dependence via its dependence on the nuclear coordinates. A TDSE is proposed in this way, namely

$$\hat{H}_{BO}(\mathbf{R}^{(I)}(t))\Phi_{\mathbf{R}^{(I)}(t)}(\mathbf{r},t) = i\hbar\partial_t \Phi_{\mathbf{R}^{(I)}(t)}(\mathbf{r},t), \tag{66}$$

for the electronic wavefunction, which is, itself, dependent on the classical trajectories. As done above, a classical trajectory is labeled by the index (I). An expansion in the adiabatic basis is introduced for $\Phi_{\mathbf{R}^{(I)}(t)}(\mathbf{r},t)$,

$$\Phi_{\mathbf{R}^{(I)}(t)}(\mathbf{r},t) = \sum_k C_k(t)\varphi^{(k)}_{\mathbf{R}^{(I)}(t)}(\mathbf{r}), \tag{67}$$

and Eq. (66) yields

$$\dot{C}^{(I)}_k(t) = \frac{-i}{\hbar}\varepsilon^{(k)}_{BO}\left(\mathbf{R}^{(I)}(t)\right)C^{(I)}_l(t) - \sum_l C^{(I)}_l(t)\sum_{\nu=1}^{N_n}\frac{\mathbf{P}^{(I)}_\nu(t)}{M_\nu}\cdot\mathbf{d}_{\nu,kl}\left(\mathbf{R}^{(I)}(t)\right) \tag{68}$$

Here, the BO PES $\varepsilon^{(k)}_{BO}(\mathbf{R})$ and the nonadiabatic coupling vectors, i.e.,

$$\mathbf{d}_{\nu,kl}(\mathbf{R}) = \int d\mathbf{r}\,\varphi^{(k)^*}_{\mathbf{R}}(\mathbf{r})\nabla_\nu\varphi^{(l)}_{\mathbf{R}}(\mathbf{r}) = \left\langle\varphi^{(k)}_{\mathbf{R}}\middle|\,\nabla_\nu\varphi^{(l)}_{\mathbf{R}}\right\rangle_{\mathbf{r}}, \tag{69}$$

which are functions of the nuclear coordinates, are evaluated at the instantaneous positions along the trajectories, they thus become functions of the trajectory itself. Henceforth, a superscript (I) will be introduced to indicate this dependence on the trajectory.

The surface-hopping scheme takes its name from the idea suggested for the evolution of the classical nuclear trajectories, namely that a trajectory evolves according to one adiabatic BO force, determined as (minus) the gradient of the BO potential energy surface (PES), until a stochastic hop occurs onto another BO PES. The classical (surface-hopping) force can then be written as

$$\mathbf{F}^{(I)}_\nu(t) = -\nabla_\nu\varepsilon^*_{BO}, \tag{70}$$

with the symbol * indicating that the force-state is selected stochastically at each time step. The discontinuity in the force, and thus in the potential energy, for a given trajectory, is compensated by a discontinuity in the velocity, and thus in the kinetic energy, that guarantees energy conservation. The hopping scheme fewest-switches (Tully (1990)) prescribes that the trajectory I hops from surface k to surface l according to the probability

$$\mathscr{P}_{k\to l} = \max\left[0, \frac{-2\,dt}{\left|C^{(I)}_k(t)\right|^2}\,\Re\left[C^{(I)^*}_k(t)C^{(I)}_l(t)\right]\sum_\nu\frac{\mathbf{P}^{(I)}_\nu(t)}{M_\nu}\cdot\mathbf{d}^{(I)}_{lk,\nu}\right], \tag{71}$$

with dt the integration time step.

The major drawback of the surface-hopping scheme is the (over)coherent evolution of the electronic coefficients coupled to the classical (independent) trajectories. The issue has been well-documented in the literature (Subotnik et al (2013); Bittner and Rossky (1995); Curchod and Tavernelli (2013b); Gao and Thiel (2017)), and several schemes have been proposed (Shenvi et al (2011b,a); Shenvi and Yang (2012); Subotnik and Shenvi (2011b,a); Jaeger et al (2012); Jasper and Truhlar (2007); Granucci and Persico (2007)) to cure or alleviate this shortcoming.

4.2.1 Application of Surface Hopping combined with LR-TDDFT

Surface hopping has been used to study a large number of excited-state mechanisms, and we refer the interested reader to specialized reviews Barbatti (2011); Curchod et al (2013); Persico and Granucci (2014) for a list of applications. The application presented here highlights the combination of surface hopping with LR-TDDFT (using the concepts developed in Sec. 3.2), including implicitly and explicitly the role of spin-orbit coupling as well as explicit solvent effects. Ruthenium (II) trisbipyridine, $[Ru(bpy)_3]^{2+}$, is an inorganic molecule recognized for its extremely efficient intersystem crossing process, i.e., when the molecule changes, in this particular case, from a singlet electronic state to a triplet electronic state (Cannizzo et al (2006); Gawelda et al (2006)). $[Ru(bpy)_3]^{2+}$ is initially photoexcited in a singlet metal-to-ligand-charge-transfer (^{1}MLCT) state before it rapidly relaxes among other ^{1}MLCT or ^{3}MLCT, as a result of the high density of states; the overall dynamics to the triplet states has been observed experimentally in water within a $\sim$50 fs timescale (Fig. 2).

In the first theoretical study (Tavernelli et al (2011)), the excited-state dynamics of the $[Ru(bpy)_3]^{2+}$ in water was studied by employing surface hopping with LR-TDDFT, in a QM/MM formalism where water molecules were treated classically. Intersystem-crossing events were analyzed *a posteriori*, monitoring the crossings between singlet and triplet states and evaluating spin-orbit coupling from qualitative rules. Owing to the cost of the overall dynamics, this study was limited to only two trajectories. Nevertheless, both trajectories indicated an ultrafast decay of the molecule towards triplet states in less than 50 fs, in good correlation with experimental evidences. The MLCT character of the different excited states implies that an electron moves from the central metal to one (or two, depending on the state) solvent-exposed bipyridine ligands. Hence, the simulation showed that water molecules in the first solvation shell can rapidly rearrange in a non-diffusive rotation around the hydrogen bond axis to stabilize an extra charge located on a close ligand. An explicit treatment of solvent molecules is central to capture such effects as well as a proper ordering of the different electronic states.

In a more recent study (Atkins and González (2017)), surface hopping combined within LR-TDDFT was used to simulate the excited-state dynamics of $[Ru(bpy)_3]^{2+}$ in gas phase, but with the explicit treatment of spin-orbit coupling in a perturbative ZORA formalism Wang and Ziegler (2005) and a larger number (101) of trajectories. This study confirmed the ultrafast decay of the original ^{1}MLCT population towards triplet states, already at the early time of the dynamics. Horizontal intersystem crossing processes were observed, followed by ultrafast nonadiabatic dynamics among the triplet states (Fig. 3). Thanks to normal-mode and principal component analysis, the authors could identify that the motion of both the ruthenium and the coordinated nitrogens is activated, even within such short timescale, leading potentially to the intersystem crossing events.

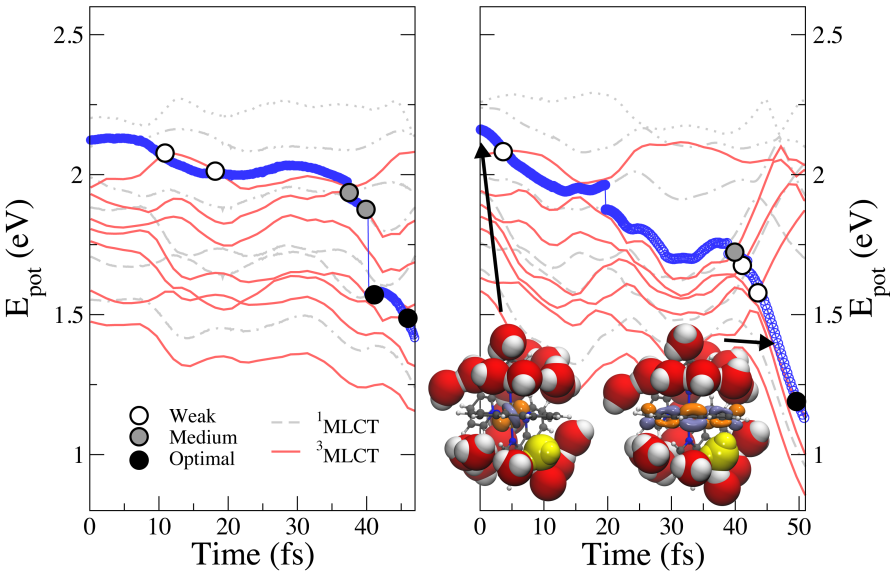

Fig. 2: Two surface hopping trajectories for $[Ru(bpy)_3]^{2+}$ in water. The driving state is highlighted with blue circles, while the 7 singlet excited states considered in the surface hopping dynamics are represented by gray dashed lines, and the 7 triplet states by red continuous lines. Filled circles indicate the analyzed crossings between singlet and triplet states, using the following color coding: white = weak, gray = medium, and black = optimal SOC strength. The inset provides a ball-and-stick representation of the $[Ru(bpy)_3]^{2+}$ molecule with part of its first water solvation shell of water molecules for two selected frames (black arrows), highlighting the fast rotation of a classical water molecule (in yellow) occurring during the dynamics. Adapted from Chemical Physics, 391, I. Tavernelli, B. F. E. Curchod, U. Rothlisberger, Nonadiabatic molecular dynamics with solvent effects: A LR-TDDFT QM/MM study of ruthenium (II) tris (bipyridine) in water, 101, Copyright (2011), with permission from Elsevier.

4.3 Coupled-trajectory mixed quantum-classical scheme

Within the Exact Factorization formalism, a trajectory-based solution of the electronic (11) and nuclear (12) equations is constructed by (i) determining the classical limit of the nuclear equation, thus deriving the corresponding Newton's equation with forces computed from the time-dependent vector $\mathbf{A}_v(\mathbf{R},t)$ and scalar $\varepsilon(\mathbf{R},t)$ potentials, (ii) introducing the Born-Huang-like expansion of Eq. (16) of the electronic wavefunction, (iii) approximating the explicit dependence on the nuclear wavefunction, i.e., the term $-i\hbar\nabla_v\chi(\mathbf{R},t)/\chi(\mathbf{R},t)$ in the definition of the coupling operator $\hat{U}_{en}^{coup}[\Phi_{\mathbf{R}},\chi]$ (13) employing information obtained from the trajectories. A thorough account of the steps adopted for the derivation of the algorithm is given

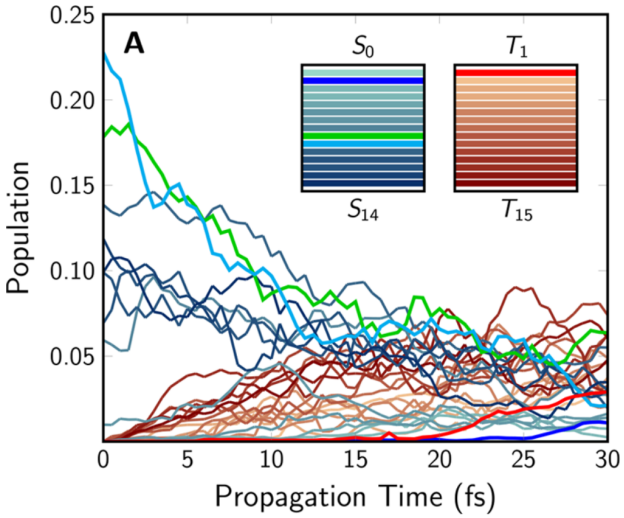

Fig. 3: Population trace of singlet (bluish) and triplet (brownish) states over 30 fs of surface hopping (population of the three sublevels of each triplet are summed together). Adapted with permission from Atkins AJ, González L (2017) Trajectory surface-hopping dynamics including intersystem crossing in $[Ru(bpy)_3]^{2+}$. The Journal of Physical Chemistry Letters 8(16):3840-3845. Copyright (2017) American Chemical Society.

in (Agostini et al (2016)). Following this procedure, the electronic and nuclear equations of the Exact Factorization can be rewritten as

$$\dot{C}_l^{(I)}(t) = \dot{C}_{\text{Eh.}\,l}^{(I)}(t) + \dot{C}_{\text{qm}\,l}^{(I)}(t) \tag{72}$$

$$\mathbf{F}_\nu^{(I)}(t) = \mathbf{F}_{\text{Eh.}\,\nu}^{(I)}(t) + \mathbf{F}_{\text{qm}\,\nu}^{(I)}(t)\,. \tag{73}$$

The electronic equation yields a set of ordinary differential equations $\dot{C}_l^{(I)}(t)$ for the expansion coefficients in the Born-Huang expansion, each labeled by a superscript (I) indicating that they are calculated along the $I-$th classical trajectory. The nuclear equation allows one to identify the classical force $\mathbf{F}_\nu^{(I)}(t)$ acting on the $\nu-$th nucleus that evolves along the $I-$th trajectory. Both equations can be decomposed as the sum of two terms: the first, indicated by Eh., comprises Ehrenfest-like terms, while the second, qm, originates from the Exact Factorization. These last terms depend on the so-called "quantum momentum", whose expression is given below. The Ehrenfest-like terms are

$$\dot{C}^{(I)}_{\mathrm{Eh.}\,l}(t) = \frac{-i}{\hbar}\varepsilon^{(l)(I)}_{BO} C^{(I)}_l(t) - \sum_k C^{(I)}_k(t) \sum_{\nu=1}^{N_n} \frac{\mathbf{P}^{(I)}_\nu(t)}{M_\nu} \cdot \mathbf{d}^{(I)}_{\nu,lk} \tag{74}$$

$$\mathbf{F}^{(I)}_{\mathrm{Eh.},\nu}(t) = -\sum_k \left|C^{(I)}_l(t)\right|^2 \nabla_\nu \varepsilon^{(k),(I)}_{BO} - \sum_{k,l} C^{(I)^*}_l(t) C^{(I)}_k(t) \left(\varepsilon^{(k),(I)}_{BO} - \varepsilon^{(l),(I)}_{BO}\right) \mathbf{d}^{(I)}_{\nu,lk}, \tag{75}$$

where we introduced the symbols $\varepsilon^{(l)(I)}_{BO}$ for the electronic adiabatic potential energy surface corresponding to state l and evaluated at the position of the $I-$th trajectory, $\mathbf{d}^{(I)}_{\nu,lk}$ for the nonadiabatic coupling vectors defined as $\langle \varphi^{(l)(I)} | \nabla_\nu \varphi^{(k)(I)} \rangle_{\mathbf{r}}$, as well evaluated at the position of the trajectory I, and $\mathbf{P}^{(I)}_\nu(t)$ for the classical momentum of the $\nu-$th nucleus evolving along the $I-$th trajectory. The additional terms in Eqs. (72) and (73), namely

$$\dot{C}^{(I)}_{\mathrm{qm}\,l}(t) = -\sum_{\nu=1}^{N_n} \frac{\mathscr{Q}^{(I)}_\nu(t)}{\hbar M_\nu} \cdot \left[\sum_k \left|C^{(I)}_k(t)\right|^2 \mathbf{f}^{(I)}_{k,\nu}(t) - \mathbf{f}^{(I)}_{l,\nu}(t)\right] C^{(I)}_l(t), \tag{76}$$

$$\mathbf{F}^{(I)}_{\mathrm{qm}\,\nu}(t) = -\sum_l \left|C^{(I)}_l(t)\right|^2 \left(\sum_{\nu'=1}^{N_n} \frac{2}{\hbar M_{\nu'}} \mathscr{Q}^{(I)}_{\nu'}(t) \cdot \mathbf{f}^{(I)}_{l,\nu'}(t)\right) \left[\sum_k \left|C^{(I)}_k(t)\right|^2 \mathbf{f}^{(I)}_{k,\nu}(t) - \mathbf{f}^{(I)}_{l,\nu}(t)\right], \tag{77}$$

can be derived *only* in the context of the Exact Factorization, as they both depend on the quantum momentum (Garashchuk and Rassolov (2003)) $\mathscr{Q}^{(I)}_\nu(t) = -\hbar(\nabla_\nu |\chi^{(I)}(t)|^2)/(2|\chi^{(I)}(t)|^2)$. Here, $|\chi^{(I)}(t)|^2$ stands for the value of the nuclear density evaluated at the position of the $I-$th trajectory. The quantum momentum appears in the expression of $\hat{U}^{coup}_{en}[\Phi_{\mathbf{R}}, \chi]$ as a purely imaginary correction to the (real-valued) classical momentum. As exhaustively described in (Agostini et al (2016)), the evaluation of the quantum momentum along the $I-$th trajectory at a given time requires knowledge of the positions of all other trajectories at the same time. This peculiar feature couples the trajectories in a non-trivial manner, thus allowing for the correct description of quantum decoherence effects. The additional new quantities appearing in Eqs. (76) and (77) are the adiabatic forces accumulated over time $\mathbf{f}^{(I)}_{l,\nu}(t) = -\int^t dt' \nabla_\nu \varepsilon^{(l),(I)}_{BO}$.

The electronic structure input required in the propagation of the CT-MQC equations of motion are the Born-Oppenheimer energies and the nonadiabatic coupling vectors. Any electronic structure methods providing these quantities can therefore be used in combination with CT-MQC. In the following, we make the choice of employing LR-TDDFT.

4.3.1 Applications

As an application of the CT-MQC approach, we report the analysis presented in (Min et al (2017)) where the photoinduced ring-opening process in Oxirane (Cor-

dova et al (2007); Tapavicza et al (2008b)) triggered by the excitation from S_0 to S_2 has been investigated. Electronic-structure calculations are performed with the CPMD code using the GGA functional PBE (Perdew et al (1996)) for ground state and excited states. Linear-response TDDFT calculations are based on the Tamm-Dancoff approximation (Tamm (1945); Dancoff (1950)). The Kleinman-Bylander (Kleinman and Bylander (1982)) pseudo-potential has been used for all atom species together with a plane-wave cutoff of 70 Ry. Initial conditions, i.e., positions and momenta, have been sampled from an ab initio ground-state 2 ps trajectory at 300 K. $N_{tr} = 100$ trajectories are propagated with a time step of 0.12 fs (5 a.u.).

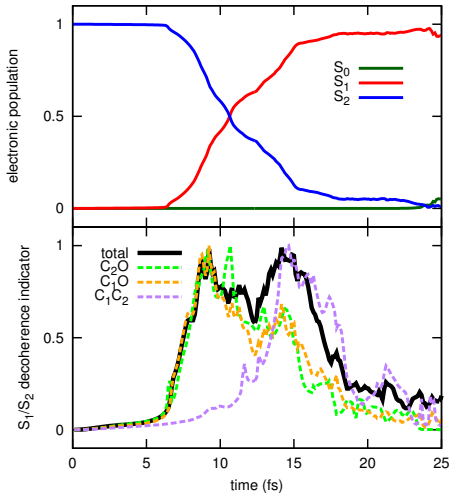

Fig. 4: Upper panel: electronic populations of S_0 (dark-green line), S_1 (red line) and S_2 (blue line) as functions of time. Lower panel: (normalized) indicator of decoherence for the element S_1/S_2 (black line), and its decomposition contributions arising from three sets of trajectories. The sets trajectories labeled by C_1O (dashed orange line) and C_2O (dashed green line) lead to a final configuration where the Oxirane ring opens via the breaking of one of the two equivalent CO bonds; the set of trajectories labeled C_1C_2 (dashed purple line) yields final configurations where the ring opens via elongation of the CC bond.

Fig. 4 shows the electronic populations (upper panel) and an indicator of decoherence (lower panel), both quantities averaged over the 100 coupled trajectories. As indicated in Eq. (72) the coefficients in the expansion of the electronic wavefunction are labeled by the trajectory index (I), therefore the average population can be determined as

$$\rho_k(t) = \frac{1}{N_{tr}} \sum_{I=1}^{N_{tr}} \left| C_k^{(I)}(t) \right|^2 \text{ for } k = 1,2\,. \tag{78}$$

Between 7 and 15 fs the trajectories cross the coupling region S_1/S_2, thus population is transferred from the initially occupied electronic state S_2 to S_1. After about 20 fs the nonadiabatic event is almost complete, and some trajectories evolving in S_1 will encounter a second coupling region S_0/S_1, as it is clearly shown by the increase of population of S_0 (and consequent decrease of population of S_1) at about 25 fs.

Similarly to Eq. (78), the indicator of decoherence introduced in (Agostini et al (2016); Min et al (2015, 2017)) is computed between the states S_1 and S_2 as an average over the trajectories,

$$\eta_{12}(t) = \frac{1}{N_{tr}} \sum_{I=1}^{N_{tr}} \left| C_1^{(I)^*}(t) C_2^{(I)}(t) \right|^2 . \tag{79}$$

The quantity $C_1^{(I)^*}(t) C_2^{(I)}(t)$ stands for the off-diagonal element of the electronic density matrix in the adiabatic representation between the first two excited states, and depend on nuclear positions through the dependence on the trajectory index (I). The decoherence indicator depends on the choice of the representation used to describe the electronic states. Our particular choice has fallen on the adiabatic representation, which is a natural choice since the dynamics is simulated in the adiabatic basis. Furthermore, this indicator of decoherence contains information simultaneously about electronic coherences and nuclear dynamics, via the parametric dependence of the adiabatic basis on the nuclear coordinates. Decoherence can thus be related to the spatial separation in configuration space of different bundles of trajectories (and thus of different wavepackets), which "loose memory" of each other while evolving along diverging paths after funnelling through the conical intersection. As abundantly discussed in the literature (Jasper et al (2006); Granucci and Persico (2007); Jaeger et al (2012); Subotnik et al (2013); Gao and Thiel (2017); Schwartz et al (1996); Fang and Hammes-Schiffer (1999); Granucci and Persico (2007); Shenvi et al (2011b,a); Shenvi and Yang (2012); Subotnik and Shenvi (2011b,a); Agostini et al (2016); Min et al (2015, 2017)), Ehrenfest dynamics and surface hopping (in their standard formulations) are not able to capture the decay of such quantity, observed here between 15 and 25 fs.

Additional information on the dynamics can be extracted from the analysis of the indicator of decoherence of Fig. 4. In fact, the pronounced double-peak structure suggests that two groups of trajectories funnel through the S_1/S_2 conical intersection at subsequent times. In order to interpret this observation, the indicator of decoherence has been decomposed in different contributions (represented by the colored curves in the lower panel of Fig. 4) arising from the different paths followed by the trajectoires after crossing the conical intersection S_1/S_2. The structures identified at the end of the simulated trajectories are (*i*) a right-open ring structure (observed with probability 36%), (*ii*) a left-open ring structure (observed with probability 47%), (*iii*) a CC-extended bond structure (observed with probability 10%), and (*iv*) a closed-ring structure (observed with probability 7%). Structures (*i*) and (*ii*) are indeed equivalent, thus the difference in the probabilities can be probably cured by improving the statistics. These structures yield the ring-opening of Oxirane via breaking of one of the two CO bonds. In structure (*iii*), the Oxirane ring opens via

the elongation of the CC bond. A few trajectories, identified as structure (*iv*), are not reactive, since the molecule more or less stays in its original configuration. If the indicator of decoherence is decomposed in contributions arising from trajectories ending in structures (*i*), (*ii*), or (*ii*), we observe that the first peak between 6 and 12 fs is produced by a first bundle of trajectories that leads to the breakage of the equivalent CO bonds. However, the $\eta_{12}(t)$ curves do not decay monotonically. Instead, the curves corresponding to the C_1O and C_2O groups both contribute to the second peak (between 12 fs and 17.5 fs). This feature indicates that the first group of trajectories is reached by a second group while funnelling through the conical intersection. The main contribution to the second peak between 12 and 16 fs is given by trajectories yielding a final CC-extended bond structure. These trajectories clearly encounter the nonadiabatic region with some delay if compared to the sets of trajectories analyzed before. Here, the indicator of decoherence is clearly single-peaked, suggesting that the corresponding trajectory bundle undergoes a transition through the S_1/S_2 conical intersection in a single step.

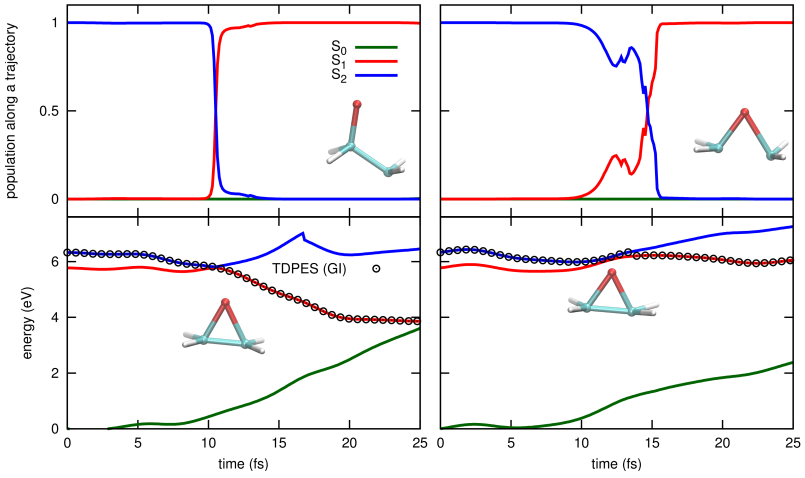

Fig. 5: Upper panels: populations of the electronic states S_0, S_1, and S_2 as functions of time for two selected trajectories of type (*i*) (left) and of type (*iii*) (right). The color code is the same used in Fig. 4. Lower panels: energy profiles (in eV) along the selected trajectories, as in the upper panels. The zero is set to be the value of the energy of S_0 at time $t = 0$ fs. In the upper panels, a ball-stick representation of Oxirane at the final time is shown, whereas in the lower panels, the configurations at the time of electronic population exchange in shown.

Observation of different final structures is related to the different paths undergone by the trajectories after crossing the S_1/S_2 region of nonadiabatic coupling. Two representative trajectories have been selected among the 100, one yielding a right-open ring structure (*i*) and one yielding a CC-extended bond configuration (*iii*). Clearly, the analysis presented for the right-open ring structure can be applied also

to the equivalent left-open ring structure (*ii*). In Fig. 5 (upper panels) we show the electronic populations $|C_k^{(I)}(t)|^2$ as functions of time and for the selected trajectories, along with the energy profiles (lower panels) of the three adiabatic states considered here and the gauge-invariant (GI) part of the TDPES (the first two terms on the right-hand side of Eq. (14)). The TDPES provides information about the "active" electronic state: if one wants to connect the interpretation of the dynamics based on the Exact Factorization to the standard perspective in terms of wavepackets evolving "on" different adiabatic surfaces, it is instructive to compare the TDPES with the BO PES, as done in Fig. 5 (lower panels).

The upper panels of Fig. 5 confirm that the coupling region is encountered by trajectories of type (*iii*) (right panels) at later times if compared to trajectories of type (*i*) or (*ii*) (left panels). Additionally, the S_2/S_1 population exchange is very sharp for type (*i*), and smooth for (*iii*). Observing the TDPES, we can argue that after about 5 fs, trajectories (*i*) encounter a steep S_2 potential, that directs them towards the conical intersection. Trajectories (*iii*) are trapped in a region of flat potential, that prevents them from a fast de-excitation to S_1. Subsequently, very different paths are undertaken, and thus different region of the S_1 PES are explored. Towards the end of the simulated dynamics, only trajectories of type (*i*) are expected to relax to the ground state S_0, as confirmed by the closing of the energy gap between S_0 and S_1 at 25 fs (lower left panel of Fig. 5). At this time, the trajectory of type (*iii*) is evolving on a portion of the BO PES S_1 that is located at about 4 eV from the ground state.

4.4 Full and Ab Initio Multiple Spawning

4.4.1 Full Multiple Spawning

Full multiple spawning (FMS) (Martínez et al (1996); Martínez and Levine (1997); Ben-Nun and Martínez (1998); Ben-Nun et al (2000); Hack et al (2001); Ben-Nun and Martínez (2002); Virshup et al (2008)) proposes to expand the nuclear amplitudes in the Born-Huang expansion in a linear combination of frozen multidimensional Gaussian functions. (Heller (1981)) But these Gaussians functions do not form a static grid; on the contrary, they are evolving over time in both position and momentum space to better adapt to the evolution of the nuclear wavefunctions, forming a set of Trajectory Basis Functions (TBFs).

$$\Psi(\mathbf{r},\mathbf{R},t) = \sum_k \sum_I^{N_{TBFs,k}} C_I^{(k)}(t)\tilde{\chi}_I^{(k)}\left(\mathbf{R};\overline{\mathbf{R}}_I^{(k)}(t),\overline{\mathbf{P}}_I^{(k)}(t),\overline{\gamma}_I^{(k)}(t),\alpha\right)\varphi_{\mathbf{R}}^{(k)}(\mathbf{r}), \qquad (80)$$

where $C_I^{(k)}(t)$ is the complex coefficient for the TBF I evolving on electronic state (k) (used here as a label) and $\tilde{\chi}_I^{(k)}\left(\mathbf{R};\overline{\mathbf{R}}_I^{(k)}(t),\overline{\mathbf{P}}_I^{(k)}(t),\overline{\gamma}_I^{(k)}(t),\alpha\right)$ is the travelling multidimensional Gaussian I on state (k) with mean position $\overline{\mathbf{R}}_I^{(k)}(t)$, momenta

$\overline{\mathbf{P}}_I^{(k)}(t)$, phase $\overline{\gamma}_I^{(k)}(t)$, and frozen width α. In FMS, the TBFs follow classical trajectories, i.e., $\overline{\mathbf{R}}(t)$ and $\overline{\mathbf{P}}(t)$ are propagated according to Hamilton's equation of motion (and the phase is integrated semi-classically). We note that this classical propagation of the TBFs does not imply that the method is semiclassical in itself, as the TBFs are only a support for the propagation of the nuclear wavefunctions. Indeed, in the limit of a large number of TBFs (N_{TBFs}), the FMS expansion would be exact. In fact, in the limit of an infinite number of Gaussian functions, their dynamics is redundant and we have a (infinitely fine) grid. We note that other methods were proposed where the TBFs follow Ehrenfest trajectories (Shalashilin (2009, 2010); Saita and Shalashilin (2012); Makhov et al (2017)) (multiconfiguration Ehrenfest, MCE) or quantum trajectories (Worth et al (2004); Lasorne et al (2006, 2007); Worth et al (2008); Mendive-Tapia et al (2012); Richings et al (2015)) (variational Multiconfiguration Gaussian, vMCG), as well as mixed strategies (Makhov et al (2014); Meek and Levine (2016); Izmaylov and Joubert-Doriol (2017); Joubert-Doriol et al (2017)).

One can express the time-dependent Schrdinger equation (1) in the basis of TBFs by inserting Eq. (80) in the former, left multiplying by

$$\left[\tilde{\chi}_J^{(k)}\left(\mathbf{R};\overline{\mathbf{R}}_J^{(l)}(t),\overline{\mathbf{P}}_J^{(l)}(t),\overline{\gamma}_J^{(l)}(t),\alpha\right)\varphi_{\mathbf{R}}^{(l)}(\mathbf{r})\right]^*$$

and integrating over both nuclear and electronic coordinates, leading, in atomic units, to (Ben-Nun and Martínez (2002)):

$$\frac{d}{dt}\mathbf{C}^l(t) = -i(\mathbf{S}_{ll}^{-1})\left[\left[\mathbf{H}_{ll} - i\dot{\mathbf{S}}_{ll}\right]\mathbf{C}^l + \sum_{k\neq l}\mathbf{H}_{lk}\mathbf{C}^k\right]. \tag{81}$$

for each electronic state l considered. The nonorthonormality of the Gaussian basis result in overlap matrices $\mathbf{S}_{ll}$ and $\dot{\mathbf{S}}_{ll}$, with elements $(\mathbf{S}_{ll})_{JI} = \langle\tilde{\chi}_J^{(l)}|\tilde{\chi}_I^{(l)}\rangle_{\mathbf{R}}$ and $\left(\dot{\mathbf{S}}_{ll}\right)_{JI} = \langle\tilde{\chi}_J^{(l)}|\frac{\partial}{\partial t}|\tilde{\chi}_I^{(l)}\rangle_{\mathbf{R}}$. We note that in Eq. (81) $\mathbf{S}_{lk} = \dot{\mathbf{S}}_{lk} = 0$, $\forall l \neq k$, due to the orthonormality of the electronic basis.

As mentioned earlier, the trajectories in FSSH are uncoupled. This is *not* the case in FMS and TBFs are coupled thanks to the Hamiltonian matrix $\mathbf{H}$ in Eq. (81). Let us consider the Hamitonian matrix element between two TBFs J and I evolving in adiabatic electronic states:

$$\begin{aligned}
H_{kl}^{IJ} =& \langle\tilde{\chi}_I^{(k)}|\hat{T}_{nuc}|\tilde{\chi}_J^{(l)}\rangle_{\mathbf{R}}\delta_{kl} + \langle\tilde{\chi}_I^{(k)}|\varepsilon_{BO}^{(k)}|\tilde{\chi}_J^{(l)}\rangle_{\mathbf{R}}\delta_{kl} \\
&- \langle\tilde{\chi}_I^{(k)}|\sum_{\rho=1}^{3N}\frac{1}{M_\rho}\langle\varphi_{\mathbf{R}}^{(k)}|\frac{\partial}{\partial R_\rho}|\varphi_{\mathbf{R}}^{(l)}\rangle_{\mathbf{r}}\frac{\partial}{\partial R_\rho}|\tilde{\chi}_J^{(l)}\rangle_{\mathbf{R}} \\
&- \langle\tilde{\chi}_I^{(k)}|\sum_{\rho=1}^{3N}\frac{1}{2M_\rho}\langle\varphi_{\mathbf{R}}^{(k)}|\frac{\partial^2}{\partial R_\rho^2}|\varphi_{\mathbf{R}}^{(l)}\rangle_{\mathbf{r}}|\tilde{\chi}_J^{(l)}\rangle_{\mathbf{R}}
\end{aligned} \tag{82}$$

If the two TBFs are in the same electronic state k, they will be coupled *via* the first two terms on the r.h.s of Eq. (82): the nuclear kinetic energy operator and the (adiabatic) electronic energy. If the two TBFs belong to different electronic states k and l, then a term containing the nonadiabatic coupling vectors (third term on the r.h.s) and the second-order nonadiabatic couplings (fourth term on the r.h.s of Eq. (82)) will ensure their coupling. We note that the diagonal second-order nonadiabatic couplings (also known as "Diagonal Born-Oppenheimer Correction") will contribute an additional intrastate coupling. FMS can easily incorporate additional source of couplings between TBFs like spin-orbit coupling (Curchod et al (2016b)), tunneling effects (Ben-Nun and Martínez (2000)), or an external electromagnetic field (Mignolet et al (2016)), for example.

4.4.2 Spawning algorithm

Up to this point, we have discussed the formal equations of FMS when a large number of TBFs is considered. However, FMS, as its name indicates, proposes to replace the large number of trajectory basis functions by an algorithm, coined the *spawning algorithm*, that will adapt the size of the basis set dynamically during the simulation. In other words, the spawning algorithm proposes the following alteration: $N_{TBFs} \rightarrow N_{TBFs}(t)$. In short, a TBF is evolving on a given PES and, as soon as a sizable coupling with a different electronic state is recorded, a spawning mode is triggered and will determine if, where, and when a new TBF should be created ("spawned") on the coupled state to maximize the coupling with the existing TBF and, therefore, the description of nonadiabatic transitions. Different versions of the spawning algorithm have been proposed and the interested reader is encouraged to read Refs. (Ben-Nun and Martínez (2002); Yang et al (2009)) for more information. It is perhaps important to note at this stage that the time-dependence of the number of TBFs, $N_{TBFs}(t)$, implies that the size of matrices and vectors in Eq. (81) will vary during the dynamics.

4.4.3 Ab Initio Multiple Spawning

FMS is in principle exact. However, the coupling between TBFs given in Eq. (82) implies integration, and therefore knowledge, of electronic structure properties like PESs or nonadiabatic couplings over the full nuclear configuration space. Approximations are, therefore, needed to treat molecular systems in their full dimensionality. Let us start by performing a Taylor expansion of the electronic quantity of interest (here the electronic energy for example) around the centroid position of two TBFs J and I evolving in electronic state k: $\overline{\mathbf{R}}_{JI}^{(kk)} = \frac{\overline{\mathbf{R}}_{J}^{(k)} + \overline{\mathbf{R}}_{I}^{(k)}}{2}$:

$$\varepsilon_{BO}^{(k)}(\mathbf{R}) = \varepsilon_{BO}^{(k)}(\overline{\mathbf{R}}_{JI}^{(kk)}) + \sum_{\rho}^{3N}(R_\rho - \overline{R}_{\rho,JI}^{(kk)})\frac{\partial \varepsilon_{BO}^{(k)}(\mathbf{R})}{\partial R_\rho}\Big|_{R_\rho=\overline{R}_{\rho,JI}^{(kk)}}$$
$$+ \frac{1}{2}\sum_{\rho\rho'}^{3N}(R_\rho - \overline{R}_{\rho,JI}^{(kk)})\frac{\partial^2 \varepsilon_{BO}^{(k)}(\mathbf{R})}{\partial R_\rho \partial R_{\rho'}}\Big|_{R_\rho=\overline{R}_{\rho,JI}^{(kk)},R_{\rho'}=\overline{R}_{\rho',JI}^{(kk)}}(R_{\rho'} - \overline{R}_{\rho',JI}^{(kk)}) + ...$$

Owing to the locality of Gaussian functions, one will consider that, to a good approximation, only the term of order zero can be retained; in other words $\varepsilon_{BO}^{(k)}(\mathbf{R}) \approx \varepsilon_{BO}^{(k)}(\overline{\mathbf{R}}_{JI}^{(kk)})$. (Ben-Nun and Martínez (2002)) This approximation, called the saddle-point approximation of order zero (SPA0), strongly simplifies the coupling between TBFs as the Hamiltonian matrix elements becomes

$$H_{kl}^{IJ} = \langle \tilde{\chi}_I^{(k)} | \hat{T}_{nuc} | \tilde{\chi}_J^{(l)} \rangle_{\mathbf{R}} \delta_{kl} + \varepsilon_{BO}^{(k)}(\overline{\mathbf{R}}_{IJ}^{(kk)}) \langle \tilde{\chi}_I^{(k)} | \tilde{\chi}_J^{(l)} \rangle_{\mathbf{R}} \delta_{kl}$$
$$- \sum_{\rho=1}^{3N} \frac{1}{M_\rho} \langle \varphi_{\mathbf{R}}^{(k)} | \frac{\partial}{\partial R_\rho} | \varphi_{\mathbf{R}}^{(l)} \rangle_{\mathbf{r}}|_{R_\rho=\overline{R}_{\rho,IJ}^{(kl)}} \langle \tilde{\chi}_I^{(k)} | \frac{\partial}{\partial R_\rho} | \tilde{\chi}_J^{(l)} \rangle_{\mathbf{R}} \tag{83}$$

(note that we also dropped the terms depending on second-order couplings). Hence, calculating the coupling between TBF J and I only require the extra calculation of electronic structure quantities at their mutual centroid position, which can easily be achieved in an on-the-fly dynamics scheme. The SPA0 allows to port the *in principle* exact framework of FMS to the nonadiabatic dynamics of molecules. The resulting nonadiabatic method within the SPA0 is often called Ab Initio Multiple Spawning (AIMS)[2]. AIMS has been coupled with different level of electronic structure like SA-CASSCF (Levine et al (2008)), MS-CASPT2 (Tao et al (2009)), FOMO-CASCI (Pijeau et al (2017)), or LR-TDDFT (Curchod et al (2017)).

4.4.4 Applications

AIMS has recently (Curchod et al (2017)) been interfaced with an implementation of LR-TDDFT accelerated by graphical processing units (GPUs) (Isborn et al (2011)), offering an important speed-up for the calculation of electronic energies, analytical gradients, and nonadiabatic coupling terms. The combination of AIMS and GPU-accelerated LR-TDDFT was employed to shed light on the excited-state dynamics of 4-N,N'-dimethylaminobenzonitrile (DMABN). DMABN is a molecule known to exhibit dual fluorescence depending on its environment, and it was proposed that the nature of the two emitting states is correlated with a twist of the dimethylamino (DMA) group Grabowski et al (2003) (see molecular structure in the inset of Fig. 6). However, DMABN is photoexcited into its second excited state, S_2, and relaxes to the first excited state S_1 where emission will occur at a later time. One question is

[2] We note that an additional approximation is commonly employed within AIMS – the independent first generation approximation – that approximates the initial nuclear wavepacket at time $t = 0$ by a set of independent parent TBFs, i.e., coupling between parent TBFs is neglected. Couplings between all the TBFs spawned by each parent TBF are preserved.(Ben-Nun and Martínez (2002))

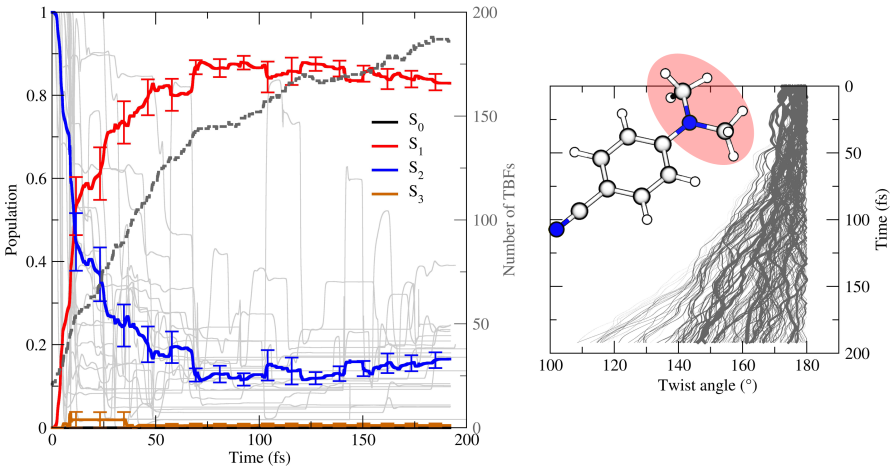

Fig. 6: Left panel: Population traces (with standard errors) of the different electronic states considered in the AIMS/LR-TDDFT dynamics. The grey dashed line indicates the number of TBFs during the dynamics. Right panel: Twist angle of the DMA group for the entire swarm of TBFs. The line width is proportional to the TBF population. Inset: representation of the DMABN molecule, with the DMA group highlighted in red. Adapted with permission from Curchod BFE , Sisto A, Martínez TJ (2016) Ab initio multiple spawning photochemical dynamics of DMABN using GPUs. The Journal of Physical Chemistry A 121(1):265-276. Copyright (2016) American Chemical Society.

then: does the S_2/S_1 nonadiabatic dynamics imply a twist of the DMA group, which could potentially have an influence on the fate of the molecule at later time in the S_1 state. Early static calculations have predicted that the S_2/S_1 transfer should be fast, and that a twist of the DMA was not required for the nonadiabatic transition to occur (Gómez et al (2005)). AIMS combined with GPU-accelerated LR-TDDFT confirmed that the S_2 population decays to S_1 in less than < 50 fs (blue line, left panel of Fig. 6). Also, the transfer of the nuclear wavepacket to S_1 is not correlated with the torsion of the DMA group, as showed by the projection of the TBFs on the twist coordinate (right panel of Fig. 6). The DMA group in fact starts its rotation only after the molecule reached S_1 ($t > 50$ fs, see right panel of Fig. 6), and such a transfer implies a change in the electronic character of the wavepacket from *charge transfer* in S_2 around the Franck-Condon region to *locally excited* after the nonadiabatic transfer to S_1. On a more technical note, the grey dashed line on the left panel of Fig. 6 indicates the number of TBFs during the AIMS dynamics. Starting from 21 parent TBFs, the spawning algorithm rapidly creates a large amount of child TBFs to ensure a good basis for the propagation in the different nonadiabatic regions encountered.

5 Conclusions

The aim of this chapter has been to provide a broad overview of quantum molecular dynamics methods to simulate nonadiabatic phenomena in isolated and condensed-phase systems, adopting a quantum-classical perspective. The combination of classical and quantum-mechanical approaches is, in fact, capable to describe, accurately and efficiently, dynamical processes involving electronic excited states. The assumption that a good description of the nuclear dynamics can be achieved based on classical mechanics is based on the fact that at the molecular scale atoms (usually heavier than a proton) are associated to a relatively short de Broglie wavelength, e.g., shorter than the typical scale of variation of the potential. Electrons, on the other hand, require a purely quantum-mechanically description, which in this work has been achieved using the framework of time-dependent density functional theory. The challenges faced in the development of theoretical and numerical approaches for nonadiabatic dynamics are copious, justifying the rise over the years of a multitude of strategies to tackle these type of problems, some of which have been described in this review chapter.

TDDFT has emerged as a very powerful method to describe electronic excited-state dynamics, both for molecular systems and in condensed phase. TDDFT describes the evolution of the electronic density in a time-dependent external potential and within the linear response regime, LR-TDDFT allows the calculation of excited-state properties, e.g., energies, forces and nonadiabatic couplings at a modest computational cost. The straightforward combination of the fundamental TDDFT theorem (leading to the time-dependent Kohn-Sham equations) with the classical motion of the nuclei gives rise to the conceptually simple Ehrenfest dynamics scheme. We described some of its applications to molecular processes involving explicit time-dependent electronic wavepacket dynamics, pointing out its limitations related to the mean-field character of the underlying approximations.

The strong interplay of electronic and nuclear motion is, however, highly non-trivial, and effects beyond the mean-field approximations are difficult to capture with trajectory-based approaches. In particular, the accurate description of the electronic "nonadiabatic effects" on the nuclear dynamics requires the derivation of a suitable theoretical framework that enables the separation of electronic and nuclear motions. Building on the TDDFT or LR-TDDFT description of the electronic dynamics within either the Born-Huang or the Exact-Factorization framework we have then reviewed three quantum-classical nonadiabatic simulation techniques that extend beyond the mean-field Ehrenfest approach, namely surface hopping, coupled-trajectory mixed quantum-classical dynamics and multiple spawning, along with some of their recent applications. The common denominator of all these techniques is that they combine "on-the-fly" trajectory-based dynamics with the computational advantages of TDDFT.

In the past years, large progresses have thus been accomplished in mixed quantum-classical nonadiabatic dynamics and we hope that this chapter will help newcomers to engage in this exciting field of research. We believe that TDDFT-based nonadiabatic dynamics can become the method of choice for treating photochemical

and photophysical processes of complex molecular systems in the gas and condensed phases. While it is hard to predict the outcome of current and future developments, the improvement of the exchange-correlation functionals, for instance going beyond the adiabatic approximation, is one of the key issues that should be addressed, aiming to get more reliable excited-state energies, nonadiabatic couplings, nuclear forces and electronic dissipation effects.Finally, the development of coupling schemes to describe the interaction with electromagnetic fields described quantum mechanically are underway (Flick et al (2017b); Dimitrov et al (2017); Flick et al (2017a)) and will open new research areas in the field of cavity quantum electrodynamics.

References

Abedi A, Maitra NT, Gross EKU (2010) Exact factorization of the time-dependent electron-nuclear wave function. Phys Rev Lett 105(12):123,002

Abedi A, Maitra NT, Gross EKU (2012) Correlated electron-nuclear dynamics: Exact factorization of the molecular wave-function. J Chem Phys 137(22):22A530

Abedi A, Agostini F, Suzuki Y, Gross EKU (2013a) Dynamical steps that bridge piecewise adiabatic shapes in the exact time-dependent potential energy surface. Phys Rev Lett 110(26):263,001

Abedi A, Maitra NT, Gross EKU (2013b) Reply to comment on "Correlated electron-nuclear dynamics: Exact factorization of the molecular wave-function". J Chem Phys 139(8):087,102

Abedi A, Agostini F, Gross EKU (2014) Mixed quantum-classical dynamics from the exact decomposition of electron-nuclear motion. Europhys Lett 106(3):33,001

Adamo C, Jacquemin D (2013) The calculations of excited-state properties with time-dependent density functional theory. Chemical Society Reviews 42(3):845–856

Agostini F, Abedi A, Suzuki Y, Gross EKU (2013) Mixed quantum-classical dynamics on the exact time-dependent potential energy surfaces: A novel perspective on non-adiabatic processes. Mol Phys 111(22-23):3625

Agostini F, Abedi A, Gross EKU (2014) Classical nuclear motion coupled to electronic non-adiabatic transitions. J Chem Phys 141(21):214,101

Agostini F, Abedi A, Suzuki Y, Min SK, Maitra NT, Gross EKU (2015a) The exact forces on classical nuclei in non-adiabatic charge transfer. J Chem Phys 142(8):084,303

Agostini F, Min SK, Gross EKU (2015b) Semiclassical analysis of the electron-nuclear coupling in electronic non-adiabatic processes. Ann Phys 527(9-10):546–555

Agostini F, Min SK, Abedi A, Gross EKU (2016) Quantum-classical non-adiabatic dynamics: Coupled- vs. independent-trajectory methods. J Chem Theory Comput 12(5):2127–2143

Agostini F, Tavernelli I, Ciccotti G (2018) Nuclear quantum effects in electronic (non)adiabatic dynamics. submitted x:xxx

Akimov AV, Prezhdo OV (2014) Advanced capabilities of the PYXAID program: Integration schemes, decoherence effects, multiexcitonic states, and field-matter interaction. Journal of Chemical Theory and Computation 10:789

Alonso JL, Clemente-Gallardo J, Echeniche-Robba P, Jover-Galtier JA (2013) Comment on "Correlated electron-nuclear dynamics: Exact factorization of the molecular wave-function". J Chem Phys 139:087,101

Andrade X, Castro A, Zueco D, Alonso J, Echenique P, Falceto F, Rubio A (2009) Modified Ehrenfest formalism for efficient large-scale ab initio molecular dynamics. J Chem Theory Comput 5(4):728–742

Atkins AJ, González L (2017) Trajectory surface-hopping dynamics including intersystem crossing in [ru (bpy) 3] 2+. The Journal of Physical Chemistry Letters 8(16):3840–3845

Baer M (2006) Beyond Born-Oppenheimer: Electronic Nonadiabatic Coupling Terms and Conical Intersections. John Wiley & Sons, Inc.

Baer R (2002) Non-adiabatic couplings by time-dependent density functional theory. Chem Phys Lett 364:75–79

Barbatti M (2011) Nonadiabatic dynamics with trajectory surface hopping method. WIREs Comput Mol Sci 1:620–633

Ben-Nun M, Martínez TJ (1998) Nonadiabatic molecular dynamics: Validation of the multiple spawning method for a multidimensional problem. J Chem Phys 108:7244–7257

Ben-Nun M, Martínez TJ (2002) Ab initio quantum molecular dynamics. Advances in Chemical Physics 121:439–512

Ben-Nun M, Martínez TJ (2000) A multiple spawning approach to tunneling dynamics. The Journal of Chemical Physics 112(14):6113–6121

Ben-Nun M, Quenneville J, Martínez TJ (2000) Ab initio multiple spawning: Photochemistry from first principles quantum molecular dynamics. J Phys Chem A 104:5161–5175

Bittner ER, Rossky PJ (1995) Quantum decoherence in mixed quantum-classical systems: Nonadiabatic processes. J Chem Phys 103:8130

Böckmann M, Doltsinis N, Marx D (2010) Unraveling a chemically enhanced photoswitch: Bridged azobenzene. Angew Chemie Int Ed 49:3382

Bonella S, Coker DF (2005) LAND-map, a linearized approach to nonadiabatic dynamics using the mapping formalism. J Chem Phys 122:194,102–13

Burghardt I, Meyer HD, Cederbaum LS (1999) Approaches to the approximate treatment of complex molecular systems by the multiconfiguration time-dependent Hartree method. J Chem Phys 111:2927

Cannizzo A, van Mourik F, Gawelda W, Zgrablic G, Bressler C, Chergui M (2006) Broadband femtosecond fluorescence spectroscopy of $[Ru(bpy)_3]^{2+}$. Angew Chem Int Ed 45:3174–3176

Car R, Parrinello M (1985) Unified approach for molecular dynamics and density-functional theory. Phys Rev Lett 55:2471

Casida M, Huix-Rotllant M (2012) Progress in time-dependent density-functional theory. Annu Rev Phys Chem 63(1):287–323, http://www.annualreviews.org/doi/pdf/10.1146/annurev-physchem-032511-143803

Casida ME (1995) Time-dependent density-functional response theory for molecules. In: Chong DP (ed) Recent Advances in Density Functional Methods, Singapore, World Scientific, p 155

Casida ME (2009) Time-dependent density-functional theory for molecules and molecular solids. J Mol Struc (Theochem) 914(1-3):3–18

Casida ME, Gutierrez F, Guan J, Gadea FX, Salahub D, Daudey JP (2000) Charge-transfer correction for improved time-dependent local density approximation excited-state potential energy curves: Analysis within the two-level model with illustration for H_2O and LiH. J Chem Phys 113:7062

Castro A, Marques MAL, Rubio A (2004) Propagators for the time-dependent Kohn-Sham equations. J Chem Phys 121(8):3425–3433, DOI 10.1063/1.1774980

Cave R, Zhang F, Maitra N, Burke K (2004) A dressed TDDFT treatment of the 2^1A_g states of butadiene and hexatriene. Chem Phys Lett 389(1):39–42

Chernyak V, Mukamel S (1996) Size-consistent quasiparticle representation of nonlinear optical susceptibilities in many-electron systems. J Chem Phys 104(2):444–459, DOI 10.1063/1.470843, URL http://link.aip.org/link/?JCP/104/444/1

Chernyak V, Mukamel S (2000) Density-matrix representation of nonadiabatic couplings in time-dependent density functional (TDDFT) theories. J Chem Phys 112:3572–3579

Cordova F, Doriol LJ, Ipatov A, Casida ME, Filippi C, Vela A (2007) Troubleshooting time-dependent density-functional theory for photochemical applications: Oxirane. J Chem Phys 127:164,111

Craig CF, Duncan WR, Prezhdo OV (2005) Trajectory surface hopping in the time-dependent kohn-sham approach for electron-nuclear dynamics. Phys Rev Lett 95:163,001

Curchod BFE, Agostini F (2017) On the dynamics through a conical intersection. J Phys Chem Lett 8:831

Curchod BFE, Tavernelli I (2013a) On trajectory-based nonadiabatic dynamics: Bohmian dynamics versus trajectory surface hopping. J Chem Phys 138:184,112

Curchod BFE, Tavernelli I (2013b) On trajectory-based nonadiabatic dynamics: Bohmian dynamics versus trajectory surface hopping. J Chem Phys 138:184,112

Curchod BFE, Tavernelli I, Rothlisberger U (2011) Trajectory-based solution of the nonadiabatic quantum dynamics equations: an on-the-fly approach for molecular dynamics simulations. Phys Chem Chem Phys 13:3231–3236

Curchod BFE, Rothlisberger U, Tavernelli I (2013) Trajectory-based nonadiabatic dynamics with time-dependent density functional theory. ChemPhysChem 14(7):1314–1340

Curchod BFE, Agostini F, Gross EKU (2016a) An exact factorization perspective on quantum interferences in nonadiabatic dynamics. J Chem Phys 145:034,103

Curchod BFE, Rauer C, Marquetand P, González L, Martínez T (2016b) Communication: Gaims–generalized ab initio multiple spawning for both internal conversion and intersystem crossing processes. The Journal of Chemical Physics 144(10):101,102

Curchod BFE, Sisto A, Martínez TJ (2017) Ab initio multiple spawning photochemical dynamics of dmabn using gpus. The Journal of Physical Chemistry A 121(1):265–276

Dancoff SM (1950) Phys Rev 78:382

Deglmann P, Furche F, Ahlrichs R (2002) An efficient implementation of second analytical derivatives for density functional methods. Chem Phys Lett 362(5-6):511 – 518, DOI 10.1016/S0009-2614(02)01084-9, URL http://www.sciencedirect.com/science/article/pii/S0009261402010849

Dimitrov T, Flick J, Ruggenthaler M, Rubio A (2017) Exact functionals for correlated electron-photon systems. New J Phys 19:113,036

Dobson JF, Bünner MJ, Gross EKU (1997) Time-dependent density functional theory beyond linear response: An exchange-correlation potential with memory. Phys Rev Lett 79(10):1905

Doltsinis NL, Marx D (2002) Nonadiabatic Car-Parrinello molecular dynamics. Phys Rev Lett 88:166,402

Dreuw A, Head-Gordon M (2004) Failure of time-dependent density functional theory for long-range charge-transfer excited states: The zincbacteriochlorin-bacteriochlorin and bacteriochlorophyll-spheroidene complexes. J Am Chem Soc 126:4007–4016

Dreuw A, Head-Gordon M (2005) Single-reference *ab initio* methods for the calculation of excited states of large molecules. Chem Rev 105:4009

Dreuw A, Weisman J, Head-Gordon M (2003) Long-range charge-transfer excited states in time-dependent density functional theory require non-local exchange. J Chem Phys 119:2943

Dunkel ER, Bonella S, Coker DF (2008) Iterative linearized approach to nonadiabatic dynamics. J Chem Phys 129:114,106

Eich FG, Agostini F (2016) The adiabatic limit of the exact factorization of the electron-nuclear wave function. J Chem Phys 145:054,110

Elliott P, Maitra NT (2012) Propagation of initially excited states in time-dependent density-functional theory. Phys Rev A 85:052,510

Elliott P, Furche F, Burke K (2009) 3 excited states from time-dependent density functional theory. Reviews in computational chemistry 26:91

Elliott P, Goldson S, Canahui C, Maitra NT (2011) Perspectives on double-excitations in TDDFT. Chem Phys 391(1):110 – 119

Epstein S (1954) Note on perturbation theory. Am J Phys 22:613

Fang JY, Hammes-Schiffer S (1999) Improvement of the internal consistency in trajectory surface hopping. J Phys Chem A 103:9399–9407

Flick J, Appel H, Ruggenthaler M, Rubio A (2017a) Cavity Born-Oppenheimer approximation for correlated electron-nuclear-photon systems. J Chem Theory Comput 13:1616–1625

Flick J, Ruggenthaler M, Appel H, Rubio A (2017b) Atoms and molecules in cavities, from weak to strong coupling in quantum-electrodynamics (QED) chemistry. Proc Nat Ac Sci 114:3026–3034

Frenkel J (1934) Wave mechanics, Clarendon, Oxford edn

Furche F (2001) On the density matrix based approach to time-dependent density functional response theory. J Chem Phys 114:5982–5992

Gaigeot MP, Lopez-Tarifa P, Martin F, Alcami M, Vuilleumier R, Tavernelli I, Hervédu Penhoat MA, Politis MF (2010) Theoretical investigation of the ultrafast dissociation of ionised biomolecules immersed in water: Direct and indirect effects. Mutat Res-Rev Mutat 704(1-3):45–53, URL http://www.sciencedirect.com/science/article/pii/S1383574210000086

Gao X, Thiel W (2017) Non-hermitian surface hopping. Phys Rev E 95:013,308

Garashchuk S, Rassolov VA (2003) Quantum dynamics with Bohmian trajectories: energy conserving approximation to the quantum potential. Chem Phys Lett 376:358

Gawelda W, Johnson M, de Groot FMF, Abela R, Bressler C, Chergui M (2006) Electronic and molecular structure of photoexcited $[Ru(II)(bpy)_3]^{2+}$ probed by picosecond x-ray absorption spectroscopy. J Am Chem Soc 128:5001–5009

Gómez I, Reguero M, Boggio-Pasqua M, Robb MA (2005) Intramolecular charge transfer in 4-aminobenzonitriles does not necessarily need the twist. Journal of the American Chemical Society 127(19):7119–7129

Grabo T, Petersilka M, Gross EKU (2000) Molecular excitation energies from time-dependent density functional theory. J Mol Struc (Theochem) 501-502:353–367

Grabowski ZR, Rotkiewicz K, Rettig W (2003) Structural changes accompanying intramolecular electron transfer: focus on twisted intramolecular charge-transfer states and structures. Chemical reviews 103(10):3899–4032

Granucci G, Persico M (2007) Critical appraisal of the fewest switches algorithm for surface hopping. J Chem Phys 126:134,114

Gritsenko O, Baerends E (2004) Asymptotic correction of the exchange–correlation kernel of time-dependent density functional theory for long-range charge-transfer excitations. J Chem Phys 121:655

Gross E, Kohn W (1990) Time-dependent density-functional theory. Advances in quantum chemistry 21:255–291

Gross EKU, Kohn W (1985) Local density-functional theory of frequency-dependent linear response. Phys Rev Lett 55:2850–2852

Gross EKU, Ullrich CA, Gossmann UJ (1994) Density functional theory of time-dependent systems. In: Gross EKU, Dreizler RM (eds) Density Functional Theory, Plenum, New York, pp 149–171

Gross EKU, Dobson J, Petersilka M (1996) Density functional theory of time-dependent phenomena. In: Nalewajski RF (ed) Density Functional Theory II, Topics in Current Chemistry, vol 181, Springer, Berlin, pp 81–172

Hack MD, Wensmann AM, Truhlar DG, Ben-Nun M, Martínez TJ (2001) Comparison of full multiple spawning, trajectory surface hopping, and converged quantum mechanics for electronically nonadiabatic dynamics. J Chem Phys 115:1172

Helgaker T, Jørgensen P (1989) Configuration-interaction energy derivatives in a fully variational formulation. Theor Chem Acc 75:111–127

Heller EJ (1981) Frozen gaussians: A very simple semiclassical approximation. The Journal of Chemical Physics 75(6):2923–2931

Hellgren M, Gross EKU (2012) Discontinuities of the exchange-correlation kernel and charge-transfer excitations in time-dependent density-functional theory. Phys Rev A 85:022,514

Hirata S, Head-Gordon M (1999) Time-dependent density functional theory within the Tamm-Dancoff approximation. Chem Phys Lett 314:291–299

Hohenberg P, Kohn W (1964) Inhomogeneous electron gas. Phys Rev B 136:B864

Hsu C, Hirata S, Head-Gordon M (2001) Excitation energies from time-dependent density functional theory for linear polyene oligomers: butadiene to decapentaene. J Phys Chem A 105(2):451–458

Hu C, Hirai H, Sugino O (2007) Nonadiabatic couplings from time-dependent density functional theory: Formulation in the Casida formalism and practical scheme within modified linear response. J Chem Phys 127:064,103

Hu C, Hirai H, Sugino O (2008) Nonadiabatic couplings from time-dependent density functional theory. II. Successes and challenges of the pseudopotential approximation. J Chem Phys 128:154,111

Hu C, Sugino O, Hirai H, Tateyama Y (2010) Nonadiabatic couplings from the Kohn-Sham derivative matrix: Formulation by time-dependent density-functional theory and evaluation in the pseudopotential framework. Phys Rev A 82(6):062,508

Hu C, Komakura R, Li Z, Watanabe K (2012) TDDFT study on quantization behaviors of nonadiabatic couplings in polyatomic systems. Int J Quantum Chem 113:263–271

Huo P, Coker DF (2012) Consistent schemes for non-adiabatic dynamics derived from partial linearized density matrix propagation. J Chem Phys 137:22A535

Hutter J (2003) Excited state nuclear forces from the Tamm-Dancoff approximation to time-dependent density functional theory within the plane wave basis set framework. J Chem Phys 118:3928–3934

Iikura H, Tsuneda T, Yanai T, Hirao K (2001) A long-range correction scheme for generalized-gradient-approximation exchange functionals. J Chem Phys 115:3540

Isborn CM, Luehr N, Ufimtsev IS, Martínez TJ (2011) Excited-state electronic structure with configuration interaction singles and Tamm–Dancoff time-dependent density functional theory on graphical processing units. J Chem Theory Comput 7(6):1814

Izmaylov AF, Joubert-Doriol L (2017) Quantum nonadiabatic cloning of entangled coherent states. The Journal of Physical Chemistry Letters 8(8):1793–1797

Jaeger HM, Fischer S, Prezhdo OV (2012) Decoherence-induced surface hopping. J Chem Phys 137:22A545

Jamorski C, Casida ME, Salahub DR (1996) Dynamic polarizabilities and excitation spectra from a molecular implementation of time-dependent density-functional response theory: N_2 as a case study. J Chem Phys 104:5134

Jasper AW, Truhlar DG (2007) Electronic decoherence time for non-born-oppenheimer trajectories. J Chem Phys 127:194,306

Jasper AW, Zhu C, Nangia S, Truhlar DG (2004) Introductory lecture: Nonadiabatic effects in chemical dynamics. Faraday Discuss 127:1

Jasper AW, Nangia S, Zhu C, Truhlar DG (2006) Non-born-oppenheimer molecular dynamics. Acc Chem Res 39:101

Joubert-Doriol L, Sivasubramanium J, Ryabinkin IG, Izmaylov AF (2017) Topologically correct quantum nonadiabatic formalism for on-the-fly dynamics. The journal of physical chemistry letters 8(2):452–456

Kapral R (2006) Progress in the theory of mixed quantum-classical dynamics. Annu Rev Phys Chem 57(1):129–157

Kapral R, Ciccotti G (1999) Mixed quantum-classical dynamics. J Chem Phys 110(18):8919–8929, DOI 10.1063/1.478811

Kleinman L, Bylander DM (1982) Efficacious form for model pseudopotentials. Phys Rev Lett 48:1425

Kurzweil Y, Baer R (2004) Time-dependent exchange-correlation current density functionals with memory. J Chem Phys 121(18):8731–8741, DOI 10.1063/1.1802793, URL `http://link.aip.org/link/?JCP/121/8731/1`

Lara-Astiaso M, Palacios A, Decleva P, Tavernelli I, Martín F (2017) Role of electron-nuclear coupled dynamics on charge migration induced by attosecond pulses in glycine. Chemical Physics Letters 683:357

Lasorne B, Bearpark MJ, Robb MA, Worth GA (2006) Direct quantum dynamics using variational multi-configuration gaussian wavepackets. Chemical physics letters 432(4):604–609

Lasorne B, Robb M, Worth G (2007) Direct quantum dynamics using variational multi-configuration gaussian wavepackets. implementation details and test case. Physical Chemistry Chemical Physics 9(25):3210–3227

Laurent AD, Jacquemin D (2013) Td-dft benchmarks: A review. International Journal of Quantum Chemistry 113(17):2019–2039

Lauvergnat D, Nauts A (2010) Torsional energy levels of nitric acid in reduced and full dimensionality with elvibrot and tnum. Phys Chem Chem Phys 12:8405

Lauvergnat D, Nauts A (2014) Quantum dynamics with sparse grids: A combination of Smolyak scheme and cubature. Application to methanol in full dimensionality. Spectrochimica Acta Part A 119:18

van Leeuwen R (1998) Causality and symmetry in time-dependent density-functional theory. Phys Rev Lett 80(6):1280–1283

van Leeuwen R (1999) Mapping from densities to potentials in time-dependent density-functional theory. Phys Rev Lett 82(19):3863–3866

Leininger T, Stoll H, Werner H, Savin A (1997) Combining long-range configuration interaction with short-range density functionals. Chem Phys Lett 275(3):151–160

Levine BG, Ko C, Quenneville J, Martinez TJ (2006) Conical intersections and double excitations in density functional theory. Mol Phys 104:1039

Levine BG, Coe JD, Virshup AM, Martinez TJ (2008) Implementation of ab initio multiple spawning in the molpro quantum chemistry package. Chemical Physics 347(1):3–16

Li X, Tully JC, Schlegel HB, Frisch MJ (2005) Ab initio Ehrenfest dynamics. J Chem Phys 123(8):084106, DOI 10.1063/1.2008258, URL http://link.aip.org/link/?JCP/123/084106/1

Li Z, Liu W (2014) First-order nonadiabatic coupling matrix elements between excited states: A lagrangian formulation at the cis, rpa, td-hf, and td-dft levels. The Journal of chemical physics 141(1):014,110

Li Z, Suo B, Liu W (2014) First order nonadiabatic coupling matrix elements between excited states: Implementation and application at the td-dft and pp-tda levels. The Journal of chemical physics 141(24):244,105

Liang W, Isborn CM, Lindsay A, Li X, Smith SM, Levis RJ (2010) Time-dependent density functional theory calculations of Ehrenfest dynamics of laser controlled dissociation of NO^+: Pulse length and sequential multiple single-photon processes. J Phys Chem A 114(21):6201–6206

Lopez-Tarifa P, Herve du Penhoat MA, Vuilleumier R, Gaigeot MP, Tavernelli I, Le Padellec A, Champeaux JP, Alcami M, Moretto-Capelle P, Martin F, Politis MF (2011) Ultrafast nonadiabatic fragmentation dynamics of doubly charged uracil in a gas phase. Phys Rev Lett 107:023,202

Lopreore CL, Wyatt RE (2002) Electronic transitions with quantum trajectories. II. J Chem Phys 116(4):1228–1238

Maitra NT (2005) Undoing static correlation: Long-range charge transfer in time-dependent density-functional theory. J Chem Phys 122:234,104

Maitra NT, Wasserman A, Burke K (2003) What is time-dependent density-functional theory? successes and challenges. In: Gonis A, Kioussis N, Ciftan M (eds) Electron Correlations and Materials Properties 2, Klewer/Plenum

Maitra NT, Zhang F, Cave RJ, Burke K (2004) Double excitations within time-dependent density functional theory linear response. J Chem Phys 120:5932

Makhov D, Symonds C, Fernandez-Alberti S, Shalashilin D (2017) Ab initio quantum direct dynamics simulations of ultrafast photochemistry with multiconfigurational ehrenfest approach. Chemical Physics

Makhov DV, Glover WJ, Martinez TJ, Shalashilin DV (2014) Ab initio multiple cloning algorithm for quantum nonadiabatic molecular dynamics. The Journal of chemical physics 141(5):054,110

Marques MAL, Maitra NT, Nogueira FMDS, Gross EKU, Rubio A (2012) Fundamentals of Time-Dependent Density Functional Theory, vol 837. Springer Verlag

Martínez TJ, Levine RD (1997) Non-adiabatic molecular dynamics: Split-operator multiple spawning with applications to photodissociation. J Chem Soc, Faraday Trans 93(5):941–947

Martínez TJ, Ben-Nun M, Levine RD (1996) Multi-electronic-state molecular dynamics: A wave function approach with applications. J Phys Chem 100(19):7884–7895

Marx D, Hutter J (2009) Ab Initio Molecular Dynamics: Basic Theory and Advanced Methods. Cambridge University Press

Meek GA, Levine BG (2016) The best of both reps—diabatized gaussians on adiabatic surfaces. J Chem Phys 145(18):184,103

Mendive-Tapia D, Lasorne B, Worth GA, Robb MA, Bearpark MJ (2012) Towards converging non-adiabatic direct dynamics calculations using frozen-width variational gaussian product basis functions. The Journal of chemical physics 137(22):22A548

Meyer HD, Worth GA (2003) Quantum molecular dynamics: propagating wavepackets and density operators using the multiconfiguration time-dependent hartree method. Theor Chim Acta 109:251

Meyer HD, Manthe U, Cederbaum LS (1990) The multi-configurational time-dependent hartree approach. Chem Phys Lett 165:73–78

Mignolet B, Curchod BFE, Martínez TJ (2016) Communication: Xfaims—external field ab initio multiple spawning for electron-nuclear dynamics triggered by short laser pulses. The Journal of chemical physics 145(19):191,104

Min SK, Agostini F, Gross EKU (2015) Coupled-trajectory quantum-classical approach to electronic decoherence in nonadiabatic processes. Phys Rev Lett 115(7):073,001

Min SK, Agostini F, Tavernelli I, Gross EKU (2017) Ab initio nonadiabatic dynamics with coupled trajectories: A rigorous approach to quantum (de)coherence. J Phys Chem Lett 8:3048

Moss CL, Isborn CM, Li X (2009) Ehrenfest dynamics with a time-dependent density-functional-theory calculation of lifetimes and resonant widths of charge-transfer states of Li^+ near an aluminum cluster surface. Phys Rev A 80:024,503, DOI 10.1103/PhysRevA.80.024503, URL http://link.aps.org/doi/10.1103/PhysRevA.80.024503

Nielsen S, Kapral R, Ciccotti G (2000) Non-adiabatic dynamics in mixed quantum-classical systems. J Stat Phys 101:225–242

Ou Q, Bellchambers GD, Furche F, Subotnik JE (2015) First-order derivative couplings between excited states from adiabatic tddft response theory. The Journal of chemical physics 142(6):064,114

Parker SM, Roy S, Furche F (2016) Unphysical divergences in response theory. The Journal of chemical physics 145(13):134,105

Perdew JP, Burke K, Ernzerhof M (1996) Generalized gradient approximation made simple. Phys Rev Lett 77:3865

Persico M, Granucci G (2014) An overview of nonadiabatic dynamics simulations methods, with focus on the direct approach versus the fitting of potential energy surfaces. Theor Chem Acc 133(9):1–28

Petersilka M, Gossmann UJ, Gross EKU (1996) Excitation energies from time-dependent density-functional theory. Phys Rev Lett 76:1212–1215

Pijeau S, Foster D, Hohenstein EG (2017) Excited-state dynamics of 2-(2?-hydroxyphenyl) benzothiazole: Ultrafast proton transfer and internal conversion. The Journal of Physical Chemistry A 121:4595

Pulay P (1987) Analytical derivative methods in quantum chemistry. Advances in Chemical Physics 69:241–286

Rappoport D, Furche F (2005) Analytical time-dependent density functional derivative methods within the RI-*J* approximation, an approach to excited states of large molecules. J Chem Phys 122(6):064105, DOI 10.1063/1.1844492, URL http://link.aip.org/link/?JCP/122/064105/1

Rassolov VA, Garashchuk S (2005) Semiclassical nonadiabatic dynamics with quantum trajectories. Phys Rev A 71(3):032,511

Requist R, Gross EKU (2016) Exact factorization-based density functional theory of electrons and nuclei. Phys Rev Lett 117:193,001

Richings G, Polyak I, Spinlove K, Worth G, Burghardt I, Lasorne B (2015) Quantum dynamics simulations using gaussian wavepackets: the vmcg method. International Reviews in Physical Chemistry 34(2):269–308

Runge E, Gross EKU (1984) Density-functional theory for time-dependent systems. Phys Rev Lett 52:997–1000

Sadri K, Lauvergnat D, Gatti F, Meyer HD (2012) Numeric kinetic energy operators for molecules in polyspherical coordinates. J Chem Phys 136:234,112

Sadri K, Lauvergnat D, Gatti F, Meyer HD (2014) Rovibrational spectroscopy using a kinetic energy operator in Eckart frame and the multi-configuration time-dependent hartree (MCTDH) approach. J Chem Phys 141:114,101

Saita K, Shalashilin DV (2012) On-the-fly ab initio molecular dynamics with multiconfigurational ehrenfest method. The Journal of chemical physics 137(22):22A506

Scherrer A, Agostini F, Sebastiani D, Gross EKU, Vuilleumier R (2015) Nuclear velocity perturbation theory for vibrational circular dichroism: An approach based on the exact factorization of the electron-nuclear wave function. J Chem Phys 143(7):074,106

Scherrer A, Agostini F, Sebastiani D, Gross EKU, Vuilleumier R (2017) On the mass of atoms in molecules: Beyond the born-oppenheimer approximation. Phys Rev X 7:031,035

Schild A, Agostini F, Gross EKU (2016) Electronic flux density beyond the born-oppenheimer approximation. J Phys Chem A 120:3316

Schwartz BJ, Bittner ER, Prezhdo OV, Rossky PJ (1996) Quantum decoherence and the isotope effect in condensed phase nonadiabatic molecular dynamics simulations. J Chem Phys 104:5942

Send R, Furche F (2010) First-order nonadiabatic couplings from time-dependent hybrid density functional response theory: Consistent formalism, implementation, and performance. J Chem Phys 132(4):044,107, DOI 10.1063/1.3292571

Shalashilin D (2009) Quantum mechanics with the basis set guided by ehrenfest trajectories: Theory and application to spin-boson model. J Chem Phys 130:244,101

Shalashilin DV (2010) Nonadiabatic dynamics with the help of multiconfigurational ehrenfest method: Improved theory and fully quantum 24d simulation of pyrazine. The Journal of chemical physics 132(24):244,111

Shenvi N, Yang W (2012) Achieving partial decoherence in surface hopping through phase correction. J Chem Phys 137:22A528

Shenvi N, Subotnik JE, Yang W (2011a) Phase-corrected surface hopping: Correcting the phase evolution of the electronic wavefunction. J Chem Phys 135:024,101

Shenvi N, Subotnik JE, Yang W (2011b) Simultaneous-trajectory surface hopping: A parameter-free algorithm for implementing decoherence in nonadiabatic dynamics. J Chem Phys 134:144,102

Stratmann RE, Scuseria GE, Frisch MJ (1998) An efficient implementation of time-dependent density-functional theory for the calculation of excitation energies of large molecules. The Journal of Chemical Physics 109(19):8218–8224

Subotnik JE, Shenvi N (2011a) Decoherence and surface hopping: When can averaging over initial conditions help capture the effects of wave packet separation? J Chem Phys 134:244,114

Subotnik JE, Shenvi N (2011b) A new approach to decoherence and momentum rescaling in the surface hopping algorithm. J Chem Phys 134:024,105

Subotnik JE, Ouyang W, Landry BR (2013) Can we derive Tully's surface-hopping algorithm from the semiclassical quantum Liouville equation? Almost, but only with decoherence. J Chem Phys 139:214,107

Suzuki Y, Watanabe K (2016) Bohmian mechanics in the exact factorization of electron-nuclear wave functions. Phys Rev A 94:032,517

Suzuki Y, Abedi A, Maitra NT, Gross EKU (2015) Laser-induced electron localization in H_2^+: Mixed quantum-classical dynamics based on the exact time-dependent potential energy surface. Phys Chem Chem Phys 17:29,271–29,280

Tamm I (1945) J Phys 9:449

Tao H, Levine BG, Martínez TJ (2009) Ab initio multiple spawning dynamics using multi-state second-order perturbation theory. J Chem Phys A 113(49):13,656–13,662

Tapavicza E, Tavernelli I, Rothlisberger U (2007a) Trajectory surface hopping within linear response time-dependent density-functional theory. Phys Rev Lett 98:023,001

Tapavicza E, Tavernelli I, Rothlisberger U (2007b) Trajectory surface hopping within linear response time-dependent density-functional theory. Phys Rev Lett 98:023,001

Tapavicza E, Tavernelli I, Rothlisberger U, Filippi C, Casida ME (2008a) Mixed time-dependent density-functional theory/classical trajectory surface hopping study of oxirane photochemistry. J Chem Phys 129:124,108

Tapavicza E, Tavernelli I, Rothlisberger U, Filippi C, Casida ME (2008b) Mixed time-dependent density-functional theory/classical trajectory surface hopping study of oxirane photochemistry. J Chem Phys 129:124,108

Tavernelli I (2006) Electronic density response of liquid water using time-dependent density functional theory. Phys Rev B 73:094,204

Tavernelli I (2013) Ab initio–driven trajectory-based nuclear quantum dynamics in phase space. Phys Rev A 87(4):042,501

Tavernelli I (2015) Nonadiabatic molecular dynamics simulations: Synergies between theory and experiments. Acc Chem Res 48(3):792–800

Tavernelli I, Röhrig U, Rothlisberger U (2005) Molecular dynamics in electronically excited states using time-dependent density functional theory. Mol Phys 103(6-8):963–981

Tavernelli I, Curchod BFE, Rothlisberger U (2009a) On nonadiabatic coupling vectors in time-dependent density functional theory. J Chem Phys 131:196,101

Tavernelli I, Tapavicza E, Rothlisberger U (2009b) Nonadiabatic coupling vectors within linear response time-dependent density functional theory. J Chem Phys 130:124,107

Tavernelli I, Curchod BFE, Laktionov A, Rothlisberger U (2010) Nonadiabatic coupling vectors for excited states within time-dependent density functional theory and beyond. J Chem Phys 133:194,104–10

Tavernelli I, Curchod BFE, Rothlisberger U (2011) Nonadiabatic molecular dynamics with solvent effects: a LR-TDDFT QM/MM study of ruthenium (II) tris (bipyridine) in water. Chem Phys 391:101

Tozer D (2003) Relationship between long-range charge-transfer excitation energy error and integer discontinuity in Kohn–Sham theory. J Chem Phys 119:12,697

Tozer DJ, Handy NC (2000) On the determination of excitation energies using density functional theory. Physical Chemistry Chemical Physics 2(10):2117–2121

Tully JC (1990) Molecular dynamics with electronic transitions. J Chem Phys 93:1061

Tully JC (1998) Mixed quantum-classical dynamics. Faraday Discuss 110:407

Ullrich CA (2012) Time-Dependent Density-Functional Theory. Oxford University Press

Ullrich CA, Tokatly IV (2006) Nonadiabatic electron dynamics in time-dependent density-functional theory. Phys Rev B 73:235,102, DOI 10.1103/PhysRevB.73.235102, URL `http://link.aps.org/doi/10.1103/PhysRevB.73.235102`

Vacher M, Bearpark MJ, Robb MA, Malhado JP (2017) Electron dynamics upon ionization of polyatomic molecules: Coupling to quantum nuclear motion and decoherence. Physical Review Letters 118(8):083,001

Van Vleck JH (1928) The correspondence principle in the statistical interpretation of quantum mechanics. Proceedings of the National Academy of Sciences of the United States of America 14(2):178

Vignale G (2008) Real-time resolution of the causality paradox of time-dependent density-functional theory. Phys Rev A 77(6):062,511

Virshup AM, Punwong C, Pogorelov TV, Lindquist BA, Ko C, Martínez TJ (2008) Photodynamics in complex environments: Ab initio multiple spawning quantum mechanical/molecular mechanical dynamics. J Phys Chem B 113(11):3280–3291

Wang F, Ziegler T (2005) A simplified relativistic time-dependent density-functional theory formalism for the calculations of excitation energies including spin-orbit coupling effect. J Chem Phys 123(15):154,102

Wang H, Thoss M (2003) Multilayer formulation of the multiconfiguration time-dependent Hartree theory. J Chem Phys 119:1289

Wiggins P, Williams JAG, Tozer DJ (2009) Excited state surfaces in density functional theory: A new twist on an old problem. J Chem Phys 131(9):091,101

Wijewardane HO, Ullrich CA (2008) Real-time electron dynamics with exact-exchange time-dependent density-functional theory. Phys Rev Lett 100:056,404, URL http://link.aps.org/doi/10.1103/PhysRevLett.100.056404

Worth G, Robb M, Burghardt I (2004) A novel algorithm for non-adiabatic direct dynamics using variational Gaussian wavepackets. Faraday Discuss 127:307–323

Worth GA, Robb MA, Lasorne B (2008) Solving the time-dependent Schrödinger equation for nuclear motion in one step: direct dynamics of non-adiabatic systems. Molecular Physics 106(16-18):2077–2091

Wyatt RE, Lopreore CL, Parlant G (2001) Electronic transitions with quantum trajectories. J Chem Phys 114(12):5113–5116

Yagi K, Takatsuka K (2005) Nonadiabatic chemical dynamics in an intense laser field: electronic wave packet coupled with classical nuclear motions. J Chem Phys 123(22):224,103

Yanai T, Tew D, Handy N (2004) A new hybrid exchange-correlation functional using the coulomb-attenuating method (CAM-B3LYP). Chem Phys Lett 393:51

Yang S, Coe JD, Kaduk B, Martínez TJ (2009) An "optimal" spawning algorithm for adaptive basis set expansion in nonadiabatic dynamics. The Journal of chemical physics 130(13):04B606

Zangwill A, Soven P (1980) Density-functional approach to local-field effects in finite systems: Photoabsorption in the rare gases. Phys Rev A 21(5):1561